COMPOSITE COUPLING ACTION OF BEAM AND SLAB IN SHEAR WALL STRUCTURE.

A Thesis

by

HARIS MD. ROUFUN AWAL

Submitted to the Department of Civil Engineering of Bangladesh University of Engineering and Technology, Dhaka in partial fulfilment of the requirements for the degree

of

MASTER OF SCIENCE IN CIVIL ENGINEERING

March, 1986

COMPOSITE COUPLING ACTION OF BEAM AND SLAB IN SHEAR WALL STRUCTURE.

A Thesis

by

HARIS MD. ROUFUN AWAL

Approved as to style and content by:

JRChoudhury

(Dr. J.R. Choudhury) Supervisor
Professor,
Dept. of Civil Engg.,
BUET, Dhaka.

Alamgir Habib

(Dr. Alamgir Habib) Member
Professor,
Dept. of Civil Engg.,
BUET, Dhaka.

(Dr. M. Shamim Z. Bosunia) Member
Professor and Head,
Dept. of Civil Engg.,
BUET, Dhaka.

M. Chowdhury

(Dr. Mahiuddin Chowdhury) Member
Associate Professor,
Dept. of NAME,
BUET, Dhaka.

March, 1986

ACKNOWLEDGEMENTS.

The author wishes to express his heartiest gratitude and profound indebtness to Professor Jamilur Reza Choudhury for his supervision, guidance and encouragement at all stages of the work. His keen interest in this topic and valuable suggestions and advice were the sources of inspiration to the author.

The author also expresses his profound gratitude to Professor Alamgir Habib for his inspiration and guidance in completing the thesis.

The author is highly obliged to Professor M. Shamim Z. Bosunia for his encouragement and affectionate guidance in completing this work.

Sincere thanks are also due to Mr. Shamim Ahsan, Mr. Rezaul Karim, Mr. Tariq Ahmed, Mr. A.K.M. Riazul Zamil, Mr. Md. Taher Abu Saif with whom the author had many a fruitful discussion.

Gratitude is also expressed to Computer Centre staff for their co-operation in ensuring a fast turnaround of jobs submitted. The assistance of Mr. M.A. Malek and Mr. Shahiduddin in preparing the thesis is gratefully acknowledged.

ABSTRACT

This thesis deals with the effect of beams on the coupling action of slab in slab-wall structures, considering only the linear elastic behaviour.

The bending stiffness of floor slabs is calculated by the finite element method (considering both flexural and in-plane deformations) and the composite action of floor slab and beam coupling a pair of laterally loaded plane shear walls is studied. The width of slab effective as flange of the composite T-beam is evaluated in the beam-slab structures for various wall configurations. The relative influences of a range of structural parameters on the effective slab width are evaluated, and design curves are presented to facilitate their determination in practical situations. The coupling action is found to be influenced by the ratio of beam depth to slab thickness, the ratio of wall opening distance to slab width and the ratio of flange length to wall opening distance.

CONTENTS

Page

NOTATIONS

L	Corridor width
Y	Slab width
Y_e	Effective slab width
X	Length of slab
L_c	Centre to centre distance between shear walls
b	Width of beam
d	Depth of beam
t	Thickness of slab
W	Wall width
P	Applied force
M	Applied moment
A_w	Cross-sectional area of web of composite coupling beam
E	Modulus of elasticity
e	Eccentricity between beam and slab neutral axes
I_c, I_{ce}	Actual and reduced second moment of area of composite coupling beam
K	Coupling stiffness of composite coupling beam
$O(x,y,z)$	Coordinate system
δ	Relative axial displacements of coupled walls
θ	Wall ratio
ν	Poisson's ratio
$[\ ]$	A rectangular or square matrix
$\{\ \}$	A column vector
d.o.f	Degree (or degrees) of freedom
$\{\underline{d}\}$	Nodal d.o.f of an element
$\{\underline{F}\}$	Nodal load matrix of an element
$[\underline{K}]$	Stiffness matrix
$[\underline{T}]$	Transformation matrix

CHAPTER 1

INTRODUCTION

1.1 General

In general, the structural system of a building is a three-dimensional complex assemblage of various combinations of interconnected structural elements. These may be discrete members or they may be continuous assemblages. The primary functions of the structural system are to carry effectively and safely all the loads acting on the building, and eventually to transmit them to the foundation.

In the process of selecting the most suitable structural system for a tall building, several factors have to be considered and optimized in addition to the height of the building. For this complicated process, no simple clear-cut method is available. The design team must use every available means, imagination, ingenuity, previous experience, and relevant literature to arrive at the best possible solution in each particular case.

In principle, in any structural system, all of the load-resisting systems and components should be equally active and ideally should work together under all types and combinations of design loads. In other words, the parts of the structural system that primarily resist horizontal loads should be able to contribute to the resistance to vertical loads as well. This is, in fact, the case in some structural systems, and many individual components such as floor systems are common to (or merged together with) horizontal load resisting frames. Even if the two framing systems are discrete and sufficiently separate, one must always consider them as being interrelated. Consequently, their possible interactions should be taken into account.

The most efficient structural system is the one that manages to combine all the structural subsystems or components into a completely integrated system in which most of the elements take part in resisting the loads. However, this ideal case is unlikely to be fully achieved in practice, due to constraints such as efficiency and ease of assembly and construction, manufacturing of joints, economic considerations, and other requirements.

1.2 Framing Systems to Resist Horizontal Loads

An important characteristic of tallness in a building is the relative importance of the lateral load-resisting and lateral stabilizing systems. The normal lateral loads are those due to wind and earthquake. The columns of tall buildings must be stabilized or laterally supported by lateral bracing systems, and the lateral bracing system must resist deformations associated with the out-of-straightness and plumb of structural members and deformation associated with lateral forces. For low-rise and medium-rise structures, the analysis and design with respect to lateral forces has generally been merely a process of checking the vertical load-resistant system for its ability to resist lateral forces. However, for tall structures the vertical load-resisting system may not have the capacity to resist lateral forces, or even if it does, the design for lateral forces may add substantially to the structural cost.

In a broad sense there are three fundamental types of lateral resisting elements:

1. Moment resistant frames
2. Braced frames
3. Shear walls

The three fundamental elements are generally in vertical planes and may be placed in one or more of three general locations:

1. Exterior (perimeter)
2. Interior, and
3. Core.

1.2.1 Moment Resistant Frames

Moment resistant frames consist of linear, horizontal members (beams) in plane with and connected to linear, vertical member (Columns) with rigid or semirigid joints. A moment resistant frame is identified by the prominence of its flexibility due to flexure of the individual beams and columns and the rotation at their joints. The strength and stiffness of the frame are proportional to the column and beam size and inversely proportional to the story height and column spacing.

1.2.2 Braced Frames

A braced frame consists of a beam and column framework infilled with diagonal bracing. It is a system composed entirely of linear members, and is identified by its flexibility due to the shortening and lengthening of the horizontal floor members and theediagonal bracing members. This system has had wide application in structural steel buildings. The braced frame may be used internally in walls or partitions, where it creates a special problem in the fitting of the portion in and around the diagonal members. If used externally, it creats an unusal facade and unsually shaped windows, which are often not considered desirable. Its primary use has been in and around cores, where it can be placed in unseen and nonarchitectural spaces. The braced frame is a very stiff and efficient structural system, since it does not involve the flexural deformation of members.

1.2.3 Shear Walls

Shear walls may be defined as planar vertical elements distinguished by their relative thinness and substantial length. Shear walls are further identified as having few openings or penetrations, such that they have little or no flexibility due to the flexure of individual pieces of the wall. Their flexibility is generally limited to the sum of overall shear deformation and overturning flexural deformation. Shear walls may be solid or penetrated with a limited number of openings. The shear wall may or may not carry substantial gravity loads. The shear wall may be a single bearing wall, a wall connecting two or more columns, or a panel wall fitting the openings of beam column frame. The shear wall system is an efficient structural form for providing lateral strength and stiffness to high-rise buildings. The different types and layouts of shear wall are shown in Fig. 1.1.

More usually, in practical structures, the walls are interconnected through floor slabs and resist both lateral and gravity loads Fig. 1.2. The floor slabs, besides acting as horizontally rigid diaphragms to collect and distribute the lateral loads among the walls, also provide some restraint against the vertical movements and rotations of the walls. The resulting interaction between the walls and the floor slabs increases the lateral stiffness of the building and reduces the overall stress levels in the walls.

If the bending stiffness of the connecting members or their wall connections is low and they behave effectively as pinned-end links, the total wind moment at any level will be shared between the walls in proportion to their flexural rigidities, provided that they bear a constant ratio to each other throughout their height. If the walls are geometrically dissimilar, such an assumption, although used often in practice, might lead to gross errors, and it is necessary to perform a more accurate analysis e.g. space frame analysis with computer.

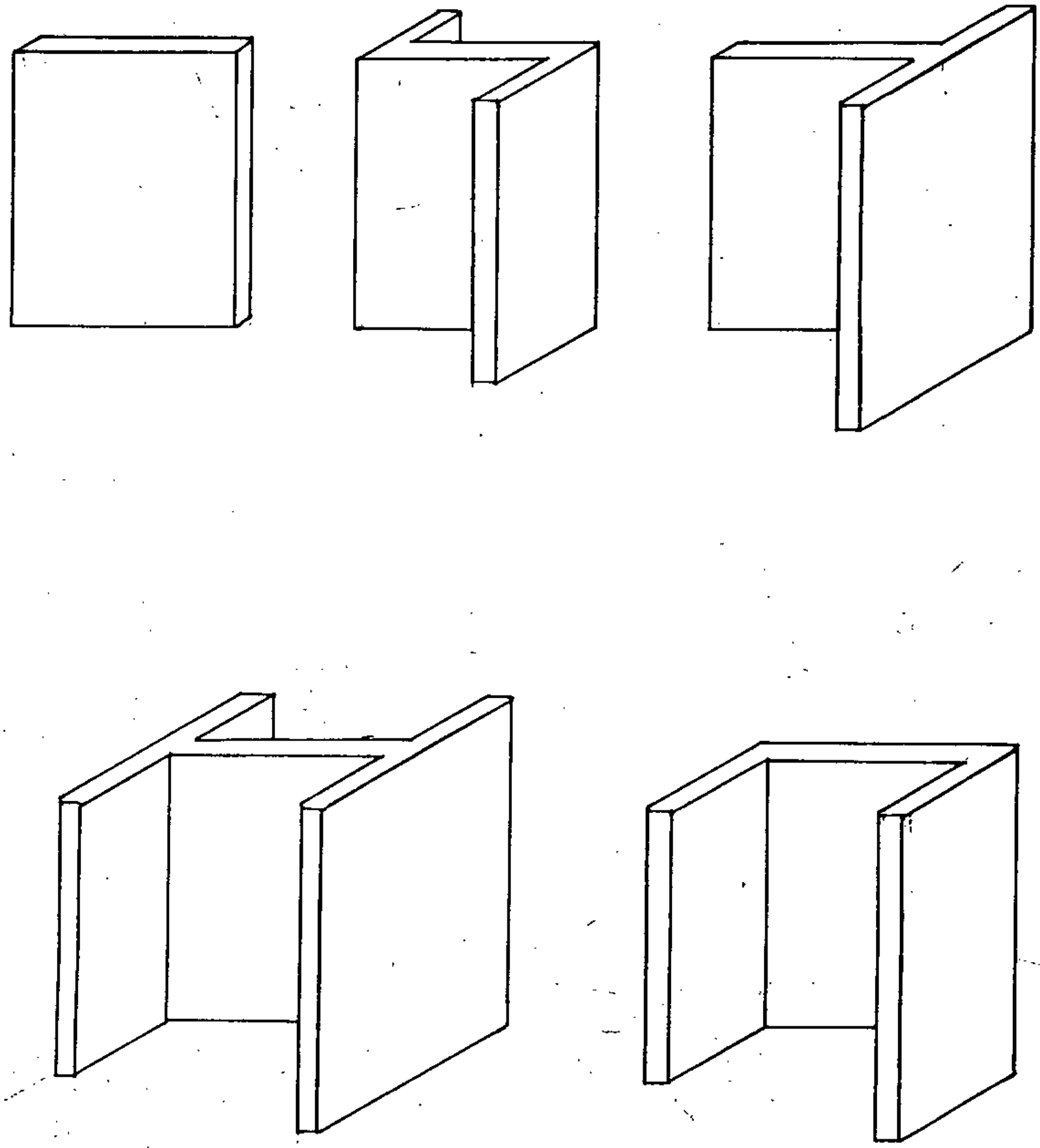

Fig. 1.1(a) Typical Shear Wall Forms.

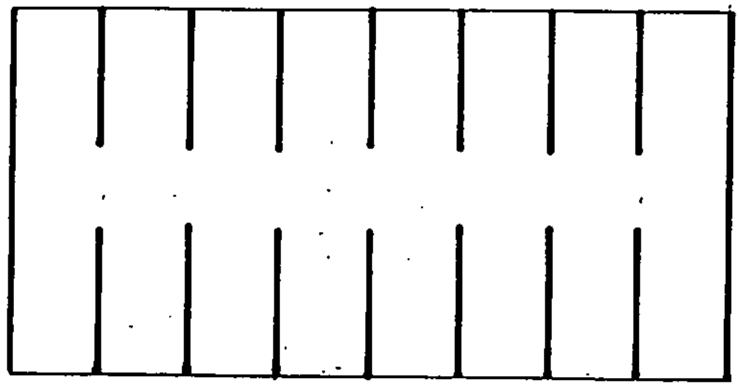

Planar Cross-Wall

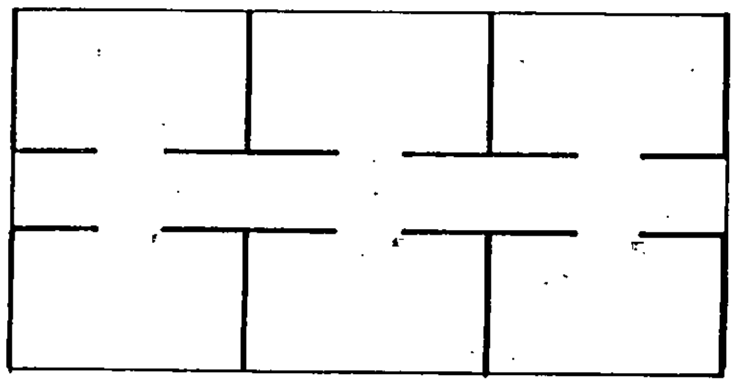

T - Shaped Cross - Wall

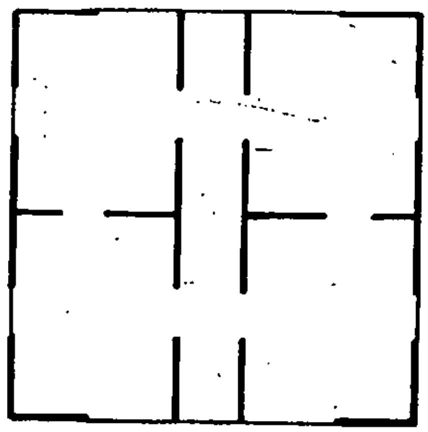

Two - Way

Fig. 1.1(b) Typical Layout of Shear Wall.

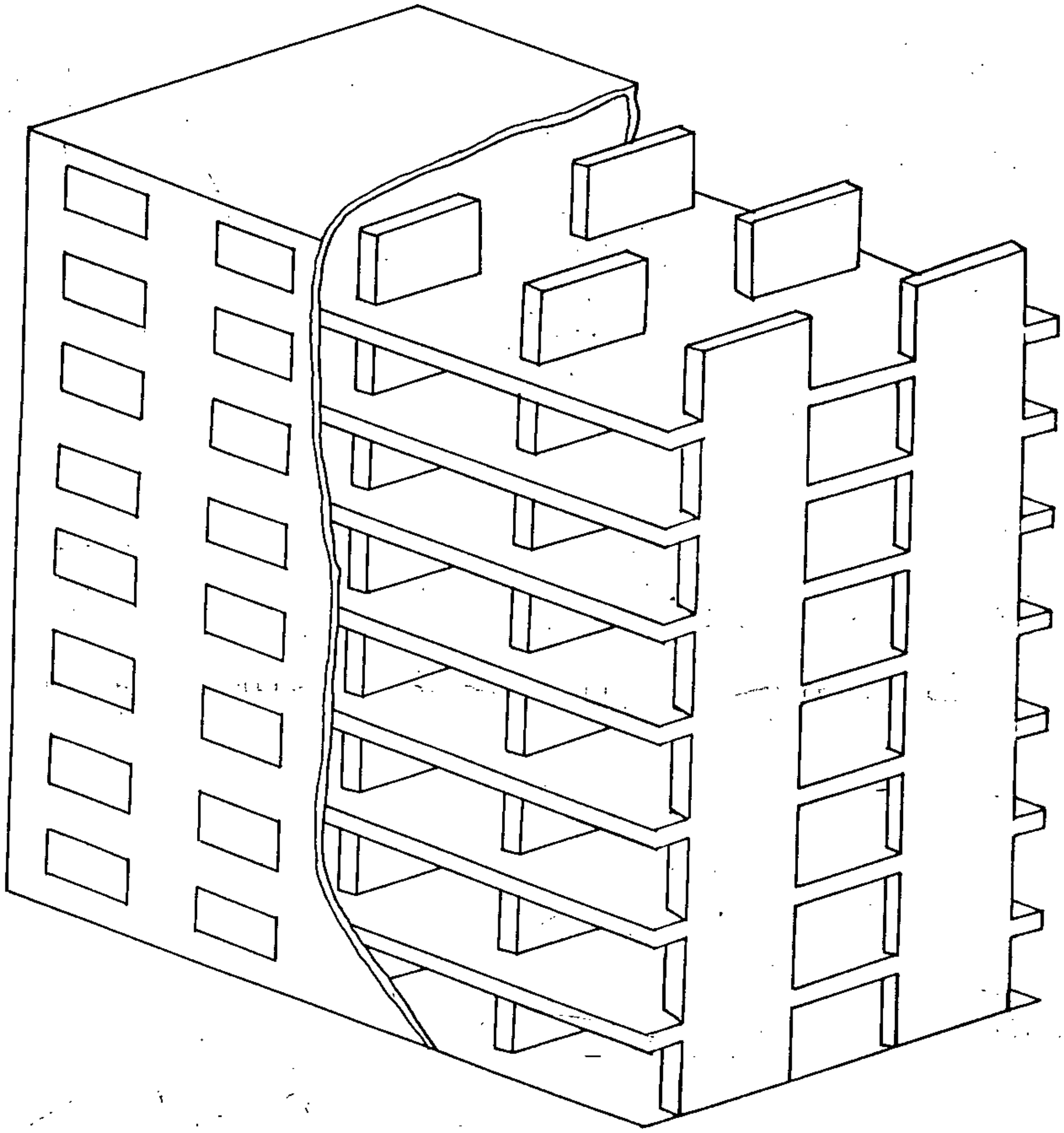

Fig.1.2 (a) Slab and Cross – Wall Building.

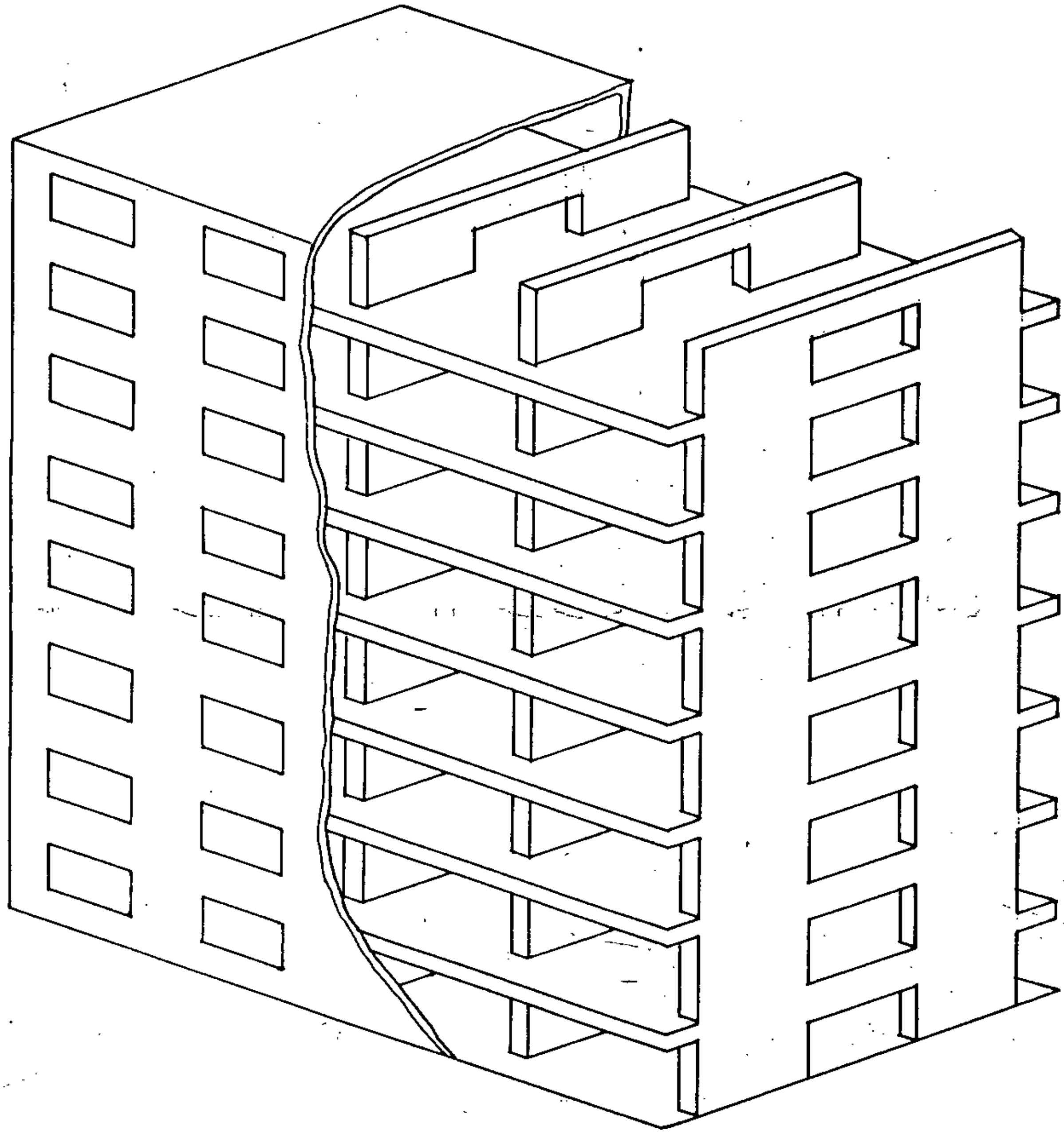

Fig. 1.2 (b) Beam - Slab and Cross - Wall Building.

The problem is complicated if, in-plane walls are joined by moment-resistant connecting members. When the walls deflect, shears and moments are induced in the connecting beams or slabs, which consequently induce axial forces in the walls. The resulting structure is much stiffer and more efficient than the pin-connected system. The effect of the finite width of a wall subjected to horizontal forces is to impose a significant vertical displacement as well as a rotation on the end of each connecting beam; this causes a much greater effective stiffness of the connecting member than in a column-supported structure.

Coupling Action of Slab

As it is not always possible to construct solid shear shear walls, pierced walls are adopted to make room for corridors and other service facilities. Now-a-days shear wall-slab structures have become very popular specially for multistoried apartment buildings. The special feature of this type of building is that the two rows of apartments are connected by a common corridor and the partition walls are treated as shear walls. As no projecting stems of beams run across the corridor, there is no need for false ceilings and the height of the buildings is appreciably shortened thus accommodating more floors in the same height.

Under the action of lateral forces the walls deflect but not as a true cantilever because of the stiffness of the slabs connecting them Fig. 1.3. Moreover, the slabs are quite useful in distributing stresses caused due to non-uniform vertical loading or differential settlement of the walls Fig. 1.3.

Effect of Beam Stiffness

Shear walls coupled by beams that are monolithic with floor slabs are frequently used in shear wall buildings. A common practice in the analysis of such coupled shear walls is to disregard the contribution of the slab and assume that the walls are coupled only by a prismatic lintel beam. However, in gravity load design it is standard practice to include a portion of the slab as a flange for the beams, so that greater moment of resistance is obtained by the composite action.

1.3 Objective of the Thesis

a) To evaluate effective flange width of the connecting beam for various wall configurations and beam depths.

b) To find the principal structural parameters that have a significant effect on effective flange width of the connecting slab.

c) To provide design guidelines for evaluating the contribution of slabs in coupling shear walls.

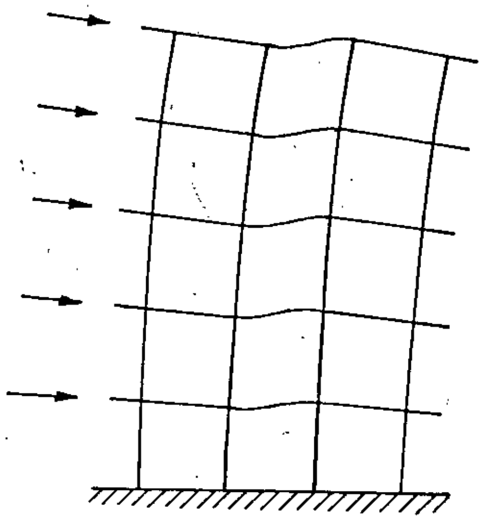

(a) Horizontal load on slab and wall structure.

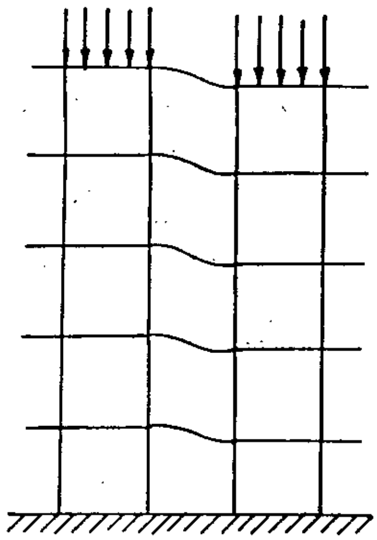

(b) Unequal Loading

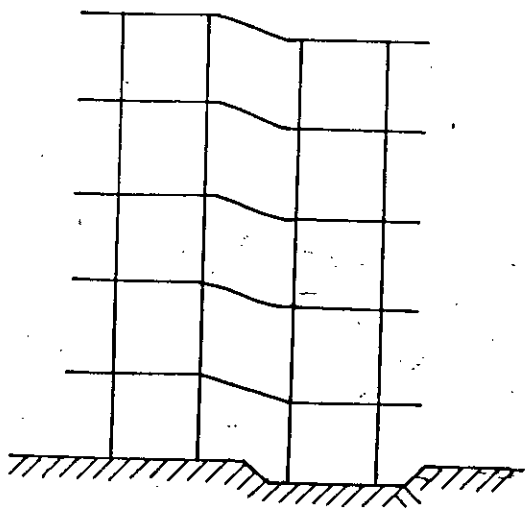

(c) Differential Settlement.

Fig. 1.3 Redistribution of Load Through Slabs

1.4 Scope of the Thesis

Scope of the thesis is restricted to the study of the-elastic behaviour of the system.

The following wall shapes have been studied:

a) A pair of planar walls.

b) A pair of T-shaped walls with flanges at the corridor edge.

c) A pair of I-shaped walls.

d) One T-shaped and another planar wall, having flanges at the corridor edge for T-shaped wall.

The analysis is carried out neglecting the influence of wall thickness. So when the ratio of wall thickness to wall opening length is very high these results may not be applied.

CHAPTER 2

REVIEW OF LITERATURE

2.1 Introduction

A typical floor system in a building consists of either:-

a) flat slabs supported only on vertical load-bearing elements (walls, columns or suspenders).

or b) slabs supported on beams which rest on walls and/or columns.

It is customary in some analyses to introduce the concept of an 'effective width of slab', which acts as a beam in flat slab-wall system or as a flange of a T-beam in a slab-beam-wall system in restraining the vertical movements of the walls. These widths are usually fixed by intuition and engineering judgement. One of the empirical guides for slabs connecting in-line pairs of wall is that if, on the plan of the slab, 45^o lines are drawn from the inner edges of the walls, then the width of the slab that lies within the points of inter-section of these lines is effective in providing bending stiffness, Fig. 2.1. Till now, the assumption regarding the value of effective width of slab varies from designer to designer and this is mostly done arbitrarily without going deep into mathematical details.

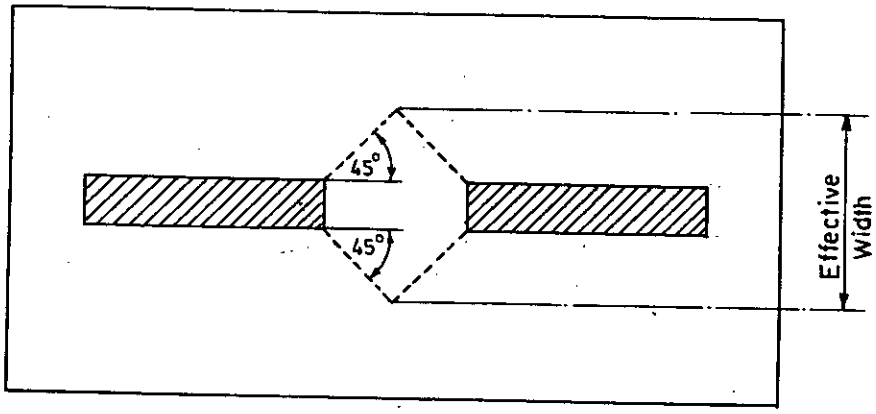

Fig. 2.1 Empirical rule for calculating effective width.

2.2 Shear Wall-Slab System

A common form of construction for multi-story apartment buildings consists of shear walls and floor slabs, in which the coupling of the cross-walls by the floor slabs has led to an efficient structural system for resisting lateral loads. The structural analysis and design of slab-coupled shear wall system may readily be performed using existing techniques for beam-coupled wall structures, provided that the equivalent width of the slab which acts effectively as a wide coupling beam, or its corresponding structural stiffness, can be assessed.

Only a limited number of research publication is available, the earliest paper being written by Khan and Sbarounis(1). They attemptedto prepare a set of suitable design curves for effective width of slab in flat slab structures. They regarded effective width as a function of width and span of slab. They also considered effective width as a function of column thickness. According to their investigation effective width increases with decreasing width/span ratio and increasing column thickness/span ratio.

Barnard and Schwaighofer(2) used Rosman theory with simplification to solve for stresses in shear walls connected solely through slabs. They assumed the entire width of the slab to be effective and verified the theoretical analysis by model tests of shear walls connected by slabs of various widths. The discussions of the same paper by Choudhury(3) Quadeer(4) and Michael(5) revealed that taking the entire slab width as effective may lead to a serious error in the calculation of stresses.

Choudhury(6) tested an asbestos cement model of a coupled shear wall structure and reached the indirect conclusion that for the particular structure, only 25% of the total width was effective. He came to the similar conclusions through an analysis of floor slabs by finite element method.

Huq(7) tested a number of steel models. He attempted to prepare a set of suitable design curves for effective width of slab in flat plate structures. He evaluated effective width for different shapes of shear walls. He also evaluated effective width as a function of corridor width and width of slab itself. According to his investigation effective width increases with increasing corridor width/slab width ratio.

Quadeer and Stafford Smith[8] analysed the slab by finite difference method and through experiments, which gave results very close to those from theoretical studies. They produced a set of curves with slab width, cantilever width, corridor width, and the width of the shear walls, as variables for effective width. Ffrom those curves it is seen that effective width is a functions of all these parameters, while a close inspection reveals that the slab widthhand corridor width have the most significant effect on the effective width. Michael[9] showed that a single curve can be drawn with all the data presented by Quadeer and Smith. He also tried to fit into it another curve, having equation $(L/Y + 0.8)(1-Y_e/Y) = 0.9$, where, L is the corridor width Y is the slab width and Y_e is the effective width of the slab.

Pulmano, Black and Kabila[10] analysed an eight-story flat slab building by finite element method. In order to verify the correctness of the approximate values of effective width of slabs, given by ACI 318-63 where full width is specified and that given by the equation presented by Michael, they analysed the equivalent frame taking the effective width of slabs as connecting beams and concluded that the latter one is nearer to the results obtained by finite element analysis.

Coull[11] tested a perspex model with closer transverse spacing of orthogonal system walls and found that the stiffening effect of the close-spaced walls upon the floor slab is a major factor in calculating the effective width of the coupling floor slabs. He also used Rosman's theory in calculating the resulting stresses which compared favourably with those obtained experimentally. He is of the opinion that in the particular type of cases the value of the effective width is greater than the full width of the slab.

The influence of orthogonal walls acting as flanges has been examined theoretically using the finite element method by Tso and Mahmoud[22]. They used finite element technique to obtain the stiffness of the slab coupled shear wall system. The configurations of the wall systems included slab coupled planar walls, T section walls, and box section core walls. There final aim was to prepare design curves in terms of the effective width of the slab between shear walls. They pointed out the fact that the additional stiffening effect from the coupling slab is significant only when the wall opening is small.

Coull and Wong[12] analysed coupled shear walls with different shear wall configuration by finite element method. They prepared sets of design curves. They investigated theoretically the variation of the effective slab width or stiffness with different geometrical layout parameters. They evaluated effective slab width as a function of wall length, slab width, wall opening width for a pair of inline plane coupled shear wall configuration. They concluded from the curves of Y_e/Y vs. W/L for the two ratios of L/Y - 0.5 and 1.5 that the effect of variation in wall length may be disregarded in the evaluation of effective slab width, so long as the influence of the ratio L/Y is considered, they recommended that the effect of dissimilar wall lengths in a pair of coupled walls may be disregarded if the ratio of the shorter wall length to the wall opening is greater than 0.5. They also concluded that the influence of slab width is strong when Y/X is smaller than L/X, but when Y/X is larger than L/X the influence of slab width diminishes rapidly. Increasing the slab width beyond a value of about three times the wall opening width appears to have virtually no effect on the effective slab width for a particular wall opening width. They showed that the influence of L/X on Y_e/X for a particular value of Y/X is almost identical to the influence of Y/X on Y_e/X for the same value of L/X. They formulated the equation of a generalized design curve as $Y_e/Y \doteq L/Y(1-0.4\ L/Y)$. They also evaluated slab width for flanged shear wall configuration and found that the presence of external wall flanges increases the effective width of the slab by less than 4% for the extreme case considered. They concluded that the influence of external wall flanges may be safely disregarded.

2.3 Shear Wall - Beams - Slab System

Shear walls coupled by lintel beams that are monolithic with floor slabs are frequently used in shear wall buildings. A common practice in the analysis of such coupled shear walls is to disregard the contribution of the slab and assume that the walls are coupled only by a prismatic beam. However, in gravity load design it is standard practice to include a portion of the slab as a flange for the beam, so that a greater moment of resistance is obtained by the composite action. While under ultimate load conditions it may be sound practice to ignore the contribution of the slab because flange sections may be cracked at points of negative bending moment, there is no reason why under working load conditions in which the structural behaviour is sensibly linearly elastic, the beneficial stiffening effect of the slab should not be included in an analysis of the coupled shear walls.

Although a number of studies have been made of the behaviour of slabs coupling shear walls, as reviewed in the preceeding article, no information had been published until 1984 when Coull and Wong[13] published their paper on the action of floor slabs acting compositively with lintel beams. They analysed the composite behaviour of a lintel and slab coupling a pair of laterally loaded shear walls by the finite element method. They evaluated the stiffening effect and the effective width of the slab acting as the flange of a composite T-beam for a range of structural parameters. The variables which were involved in the structural geometry of a typical floor panel coupling a pair of shear walls included the slab width Y, the wall opening, L, the wall length, W, the slab thickness, t, the lintel width, b, and depth, d. They found that the composite stiffness ratio and effective flange width, Y_e/Y, increased substantially with the wall opening width, L/t, over the range of values considered. The influence of wall opening width, however, tends to become less important with larger values of L/t. They also concluded that for practical purposes, the effect of variations in lintel width may be disregarded in the evaluation of effective flange width. They also found that the composite stiffness ratio decreases with an increase in lintel depth and the effective flange width on the other hand increases with lintel depth.

It is seen that the effective flange width values for the practical range of relative lintel depths considered are substantially lower than the effective width for the limiting case of a flat slab floor without lintel beam.

CHAPTER 3

THEORETICAL ANALYSIS AND PROGRAM DEVELOPMENT.

3.1 Introduction

Shear walls coupled by beams that are monolithic with floor slabs are a common type of construction for apartment buildings. The load bearing shear walls have a dual function of resisting the gravity and lateral loads, resulting in an efficient use of materials. Further savings may be achieved by taking into account the effect of coupling between shears walls by lintel beams. Depending on the plan configuration and dimensions, the floor slabs can provide substantial increase of lateral stiffness to the whole building, thus reducing the sway effect due to lateral loads.

The composite behaviour of a beam and slab coupling a pair of laterally loaded shear walls is investigated by the finite element method. The finite element method is being applied extensively in plate bending problems, since it was first used by Adini and Clough(14) and Melosh(15). Jenkins and Harrison(16) suggested the use of this method in calculating the stiffness of slabs in shear core structures. One of the major advantages in using the finite element method in the present problem is the comparative ease with which it can be incorporated into a general programme for analysing the equivalent frame which is, in essence, also a finite element procedure.

3.2 Assumptions Made in the Analysis

In order to limit the structural parameters involved to only the most significant, the investigation is limited to the study of the interior bay of a cross-wall structure, assumed to have a large number of bays in the longitudinal direction and one bay in the transverse direction.

It is assumed that under the action of lateral forces, the walls deflect equally due to the high in-plane stiffness of the floor slabs. As a result, the slopes of the walls are equal at all levels. An application of the standard slope deflection equations for prismatic beams then shows that, under these conditions, the end moments are equal and a point of contraflexure occurs at the mid span position of each beam[6]. This assumption is sufficiently accurate for design purposes, unless one wall is very small compared to the other.

A study made by Coull and Wong[12] of walls coupled by slabs alone has shown that the effects of dissimilar wall lengths may be disregarded, provided that the length of the smaller wall is greater than about half the length of opening between walls, which will be true in almost all practical situations.

3.3 Stiffness of Coupling Beam

The shear walls resist the lateral loads on the structure, due to wind or earthquake effects, by cantilever bending action, which results in rotations of wall cross-sections. The free bending of a pair of shear walls is resisted by the lintel beams together with the floor slabs, which are forced to rotate and bend out of plane where they are connected rigidly to the walls Fig. 3.1(b).

Due to the large depth of the wall, considerable differential shearing action is imposed on the connecting beam, which develops transverse reactions to resist the wall deformations Fig. 3.1(c), and induces tensile and compressive axial forces into the walls. As a result of the large lever arm involved, relatively small axial forces can give rise to substantial moments of resistance, thereby reducing greatly the wind moments in the walls, and the resulting tensile stresses at the windward edges. The lateral stiffness of the structure is also considerably increased. A similar situation arises if relative vertical deformation of the walls occurs, due to unequal vertical loading on the walls or to differential foundation settlement. The effect on the connecting beam is similar to that produced by parallel wall rotation by bending Fig. 3.1(d) and 3.1(e).

Let us consider the elastic deformation of a beam of clear span L coupling a pair of shear walls with centroidal axes distance, L_c apart undergoing parallel rotations, θ , under the actions of wind moments. M_1 and M_2 Fig. 3.2(a). As is customary in such analyses it is assumed that plane sections of the wall

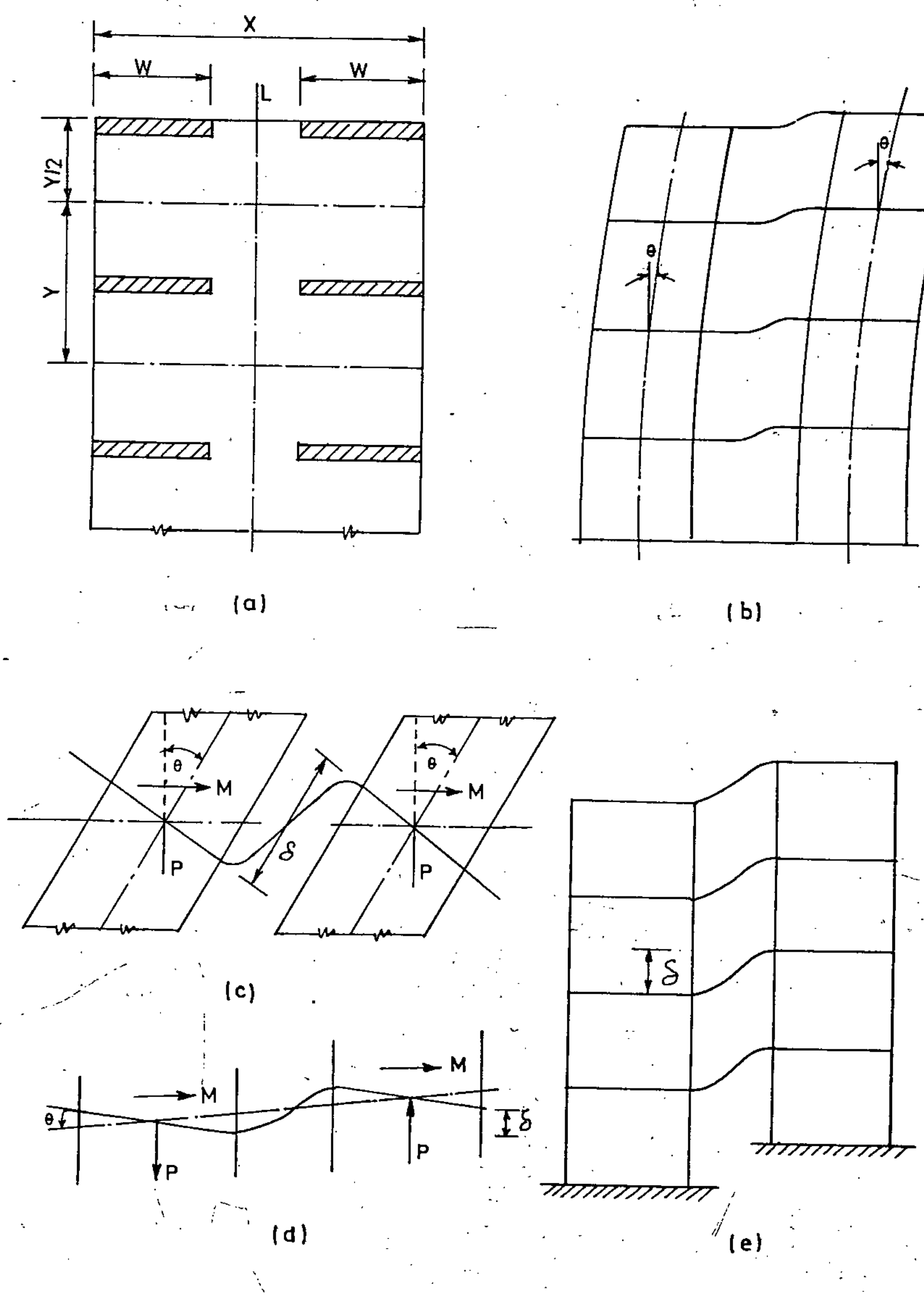

Fig. 3.1 Structural action of coupled shear wall-slab structure.

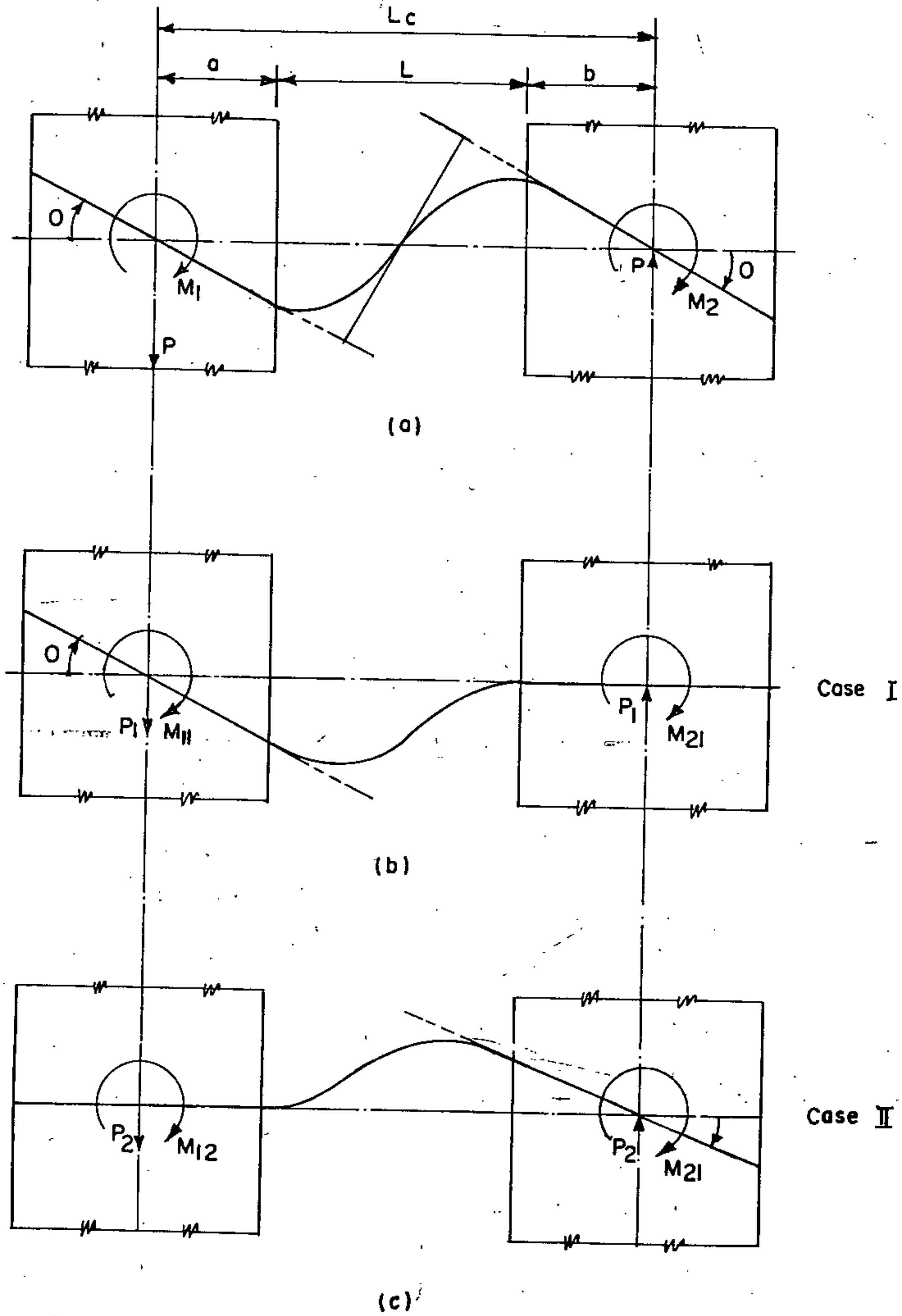

Fig. 3.2 Wall rotations as the sum of individual wall rotation.

remain plane in bending. The deformations of the walls in Fig. 3.2(a) can be viewed as the sum of the deformation in Fig. 3.2(b) and in Fig. 3.2(c).

For Case I

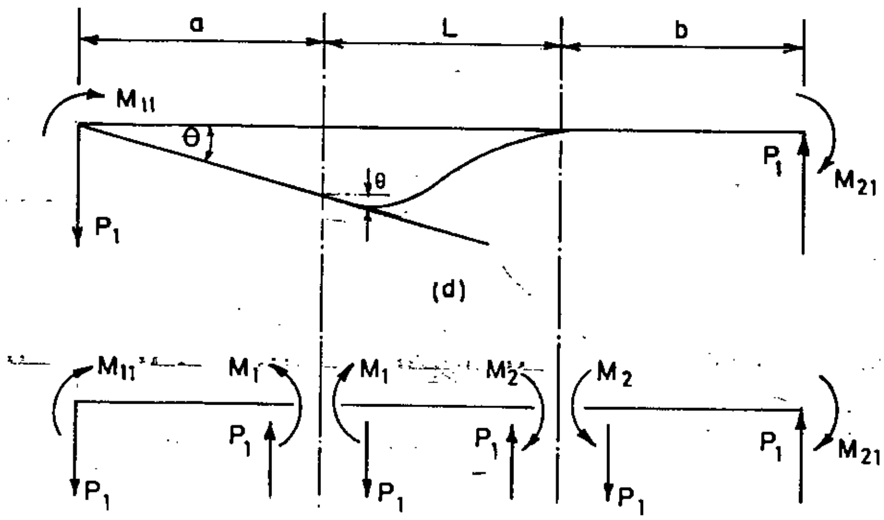

(d)

(e)

we have

$$m_1 = 4EI_e\theta/L + 6EI_e a\ \theta/L^2 \qquad 3.1$$

$$m_2 = 2EI_e\ \theta/L + 6EI_e a\ \theta/L^2 \qquad 3.2$$

$$\therefore\ P_1 = (m_1+m_2)/L = (6EI_e/L^2+12EI_e a/L^3)\ \theta \qquad 3.3$$

$$M_{11} = m_1 + aP_1 = \frac{4EI_e}{L}\left(1 + \frac{3a}{L} + \frac{3a^2}{L^2}\right)\theta \qquad 3.4$$

$$M_{21} = m_2 + bP_1 = \frac{4EI_e}{L}\left(\tfrac{1}{2} + \frac{3}{2}\ \frac{a+b}{L} + \frac{3ab}{L^2}\right)\theta \qquad 3.5$$

Similarly from Case II

$$M_{22} = \frac{4EI_e}{L}(1 + 3b/L + 3b^2/L^2)\,\theta \qquad 3.6$$

$$M_{12} = \frac{4EI_e}{L}(1/2 + 3(a+b)/2L + 3ab/L^2)\,\theta \qquad 3.7$$

$$\therefore\ M_1 = M_{11} + M_{12} = \frac{4EI_e}{L}(3/2 + 3(3a+b)/2L + 3(a^2+ab)/L^2)\,\theta$$

$$M_1 = \frac{6EI_e}{L} \cdot \frac{(L+2a)L_c}{L^2}\,\theta \qquad 3.8$$

$$\therefore\ M_1/\theta = \frac{6EI_e}{L}\ \frac{(L+2a)L_c}{L^2} \qquad 3.8a$$

and $$M_2 = \frac{4EI_e}{L}(3/2 + 3(a+3b)/2L + 3(ab+b^2)/L^2)\,\theta$$

$$\therefore\ M_2 = \frac{6EI_e}{L} \cdot \frac{(L+2b)L_c}{L^2}\,\theta \qquad 3.9$$

$$\frac{M_2}{\theta} = \frac{6EI_e}{L}\ \frac{(L+2b)L_c}{L^2} \qquad 3.9a$$

For symmetric walls, we have $a = b$

and $L + 2a = L + 2b = L_c$

and equations 3.8 and 3.9 become

$$M = M_1 = M_2 = \frac{6EI_e}{L} \cdot \frac{L_c^2}{L^2}\,\theta \qquad 3.10$$

The coupling stiffness of the beam, which may be defined in terms of the moment-rotation relationship for the wall,

$$\frac{M}{\theta} = \frac{6EI_e}{L} \left(\frac{L_c}{L} \right)^2 \tag{3.11}$$

The moment-rotation relationship for a pair of shear walls coupled by a lintel beam with the floor slab can be evaluated by a finite element analysis, allowing the effective second moment of area for the composite coupling medium to be obtained from Eq. (3.11) for equal wall lengths or either from (3.8a) or from Eq. (3.9a) for unequal wall length.

3.4 Effective Flange Width of Composite Coupling Beam[13]

In common with gravity load design, a portion of the floor slab may be assumed to act as the flange of a T-beam. Using effective second moment of area, I_e, it can be shown that the effective flange width Y_e is given by

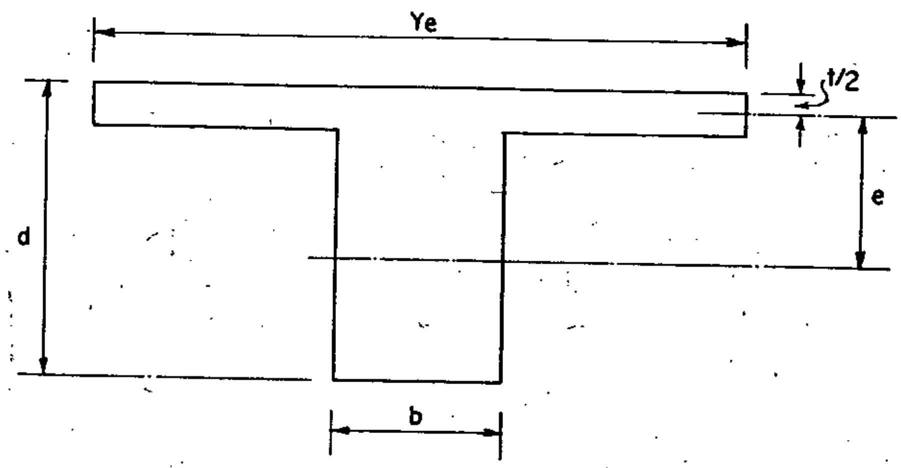

Fig. 3.3 Composite coupling beam cross-section.

$$Y_e = b + \frac{C + (C^2 + 48t^2 A_w(I_e - I_w))^{\frac{1}{2}}}{2t^3} \tag{3.12}$$

in which b = the width of the beam; t = the slab thickness $C = 12\,(I_e - I_w) - A_w\,(t^2 + 12e^2)$; e = the eccentricity between the centroids of the web and flange sections, and I_w second moment of area for the web Fig. 3.3.

3.5 Finite Element Analysis of Slab and Beam

The slab that is monolithic with the lintel beam is subjected to membrane as well as bending effects under composite coupling action. In order to model this behaviour adequately, the slab is represented by a rectangular flat shell element and beam by the beam element with degrees of freedom similar to those of shell element node. The element used is obtained by combining a standard plate bending element with three degrees of freedom at each node (transverse displacement and rotations about the x and y-axes) with a standard plane stress element with two degrees of freedom at each node (in-plane displacements in x and y-directions) so that the flexural as well as the membrane characteristics are incorporated in the same element.

For the lintel, the beam is divided into elements as shown in Fig. 3.4. From the assumptions that slab and beam acts compositely, stiffness matrices corresponding to the beam's centroidal nodes are obtained first and than transformed to the corresponding nodes of flat shell element which are assumed to be rigidly connected with the centroidal nodes of beams by rigid links.

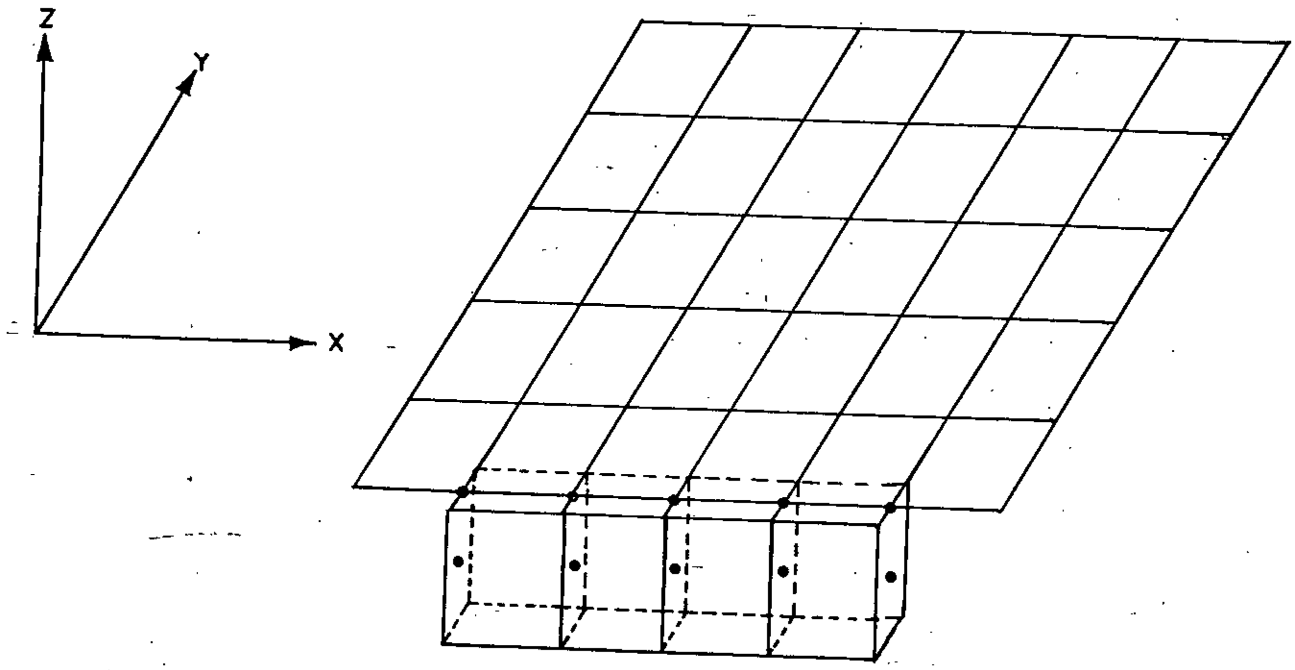

Fig. 3.4 Typical finite element idealization of Beam and floor slab.

3.5.1 Flat Elements

The classical methods for analyzing shell structures yield governing differential equations whose complexity depends greatly on shell geometry. Analytical solutions of these equations are available only for shells with simple geometric forms and for restricted boundary conditions.

The finite element method, which was introduced in the fifties, is a completely general approach for the solution of problem in stress analysis. The finite element method implies an idealization of the shell surface as an assemblage of discrete structural elements. The stiffness properties of the individual elements are evaluated from an assumed set of displacement patterns. These displacement patterns or functions should include:

1. All rigid body motions
2. Constant strain and curvature states-

Planar quadrilateral elements may be used for the analysis of shells for which groups of four surface points lying in one and the same plane can be conveniently found.

It is important to emphasize that when using planar elements, errors of a geometric nature are introduced in addition to the errors associated with the assumed displacement functions. However, these geometrical errors diminish with decreasing mesh size.

The structural idealization and its subsequent discretization is achieved by dividing the continum into a number of rectangular, triangular, quadrilateral or arbitrarily shaped elements. In the present analysis, rectangular elements have been used. Although it has been shown that rectangular elements give better results than triangular elements, the major disadvantage of these elements is the difficulty encountered in dealing with irregular, curved boundaries. Most of the shear walls are built to a rectangular module and the slabs are also regular in shape so this difficulty should not arise in analysing slab coupled with shear walls and beams.

Analysis of shell structures by the finite element method was first based on the pure membrane theory, and made use of the triangular constant strain element. However, a satisfactory shell element must contain both the plane stress and the plate bending stiffnesses. If the relative displacements for a planar shell element are small, the membrane or in-plane action and the bending action are uncoupled within each element. The stiffness matrix for the shell element may therefore be obtained by superimposing two independently derived stiffness matrices:

1. The stiffness matrix for a plane stress finite element.

2. The stiffness matrix for a plate bending finite element.

The use of flat plate elements for analysis of shells was first presented by Zienkiewicz and Cheung[17] and by Clough and Tocher[18]. It is easy to generate stiffness matrix for a flat element. The shell element has three translational and two rotational degrees of freedom of each model point, as shown in Fig. 3.5. The rotation about an axis normal to the element is not included among the nodal parameters. This may lead to some difficulties wheh transforming the element stiffness matrix to the global coordinate system. This problem may be overcome by transforming only the translational degrees of freedom to the global coordinate system. The rotational degrees of freedom were transformed to a common tangent plane at each nodal point, neglecting the rotations about the axis normal to this plane.

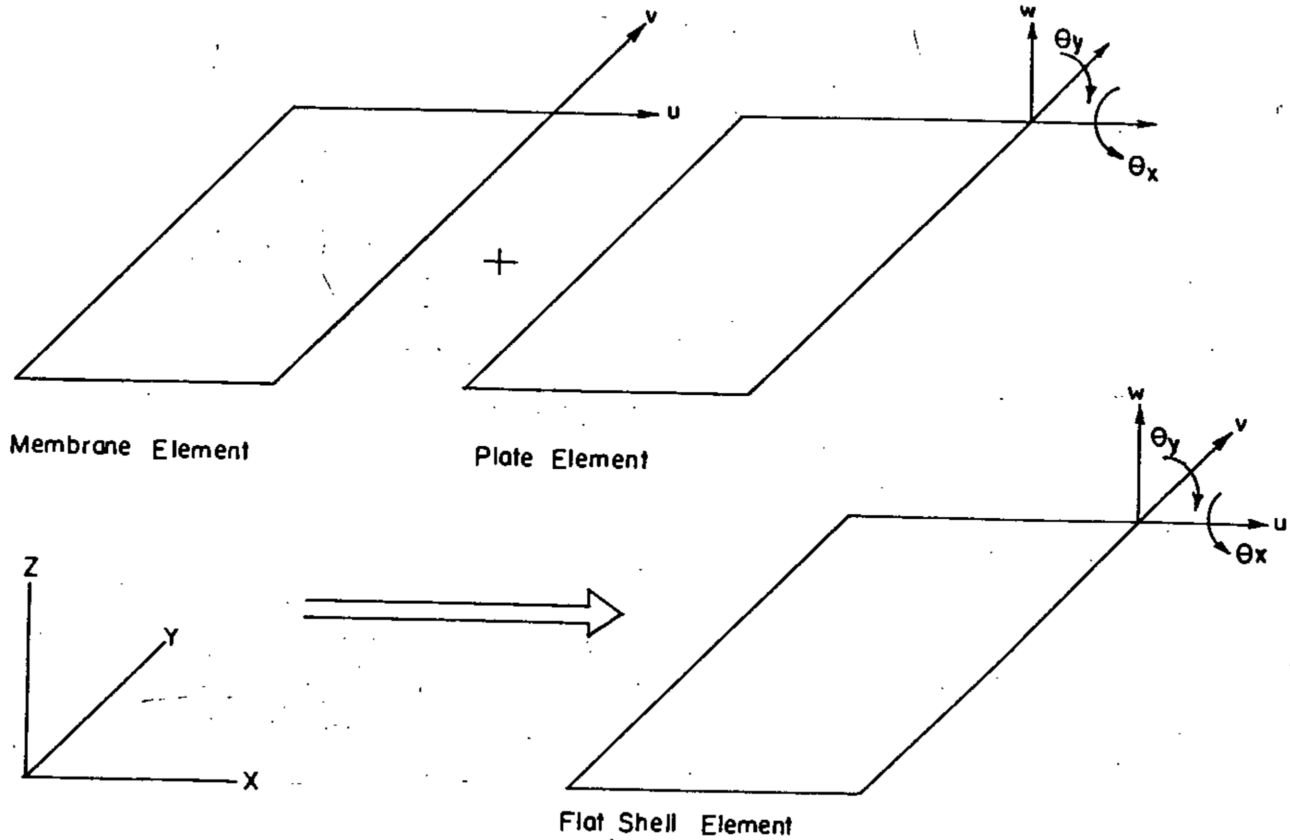

Fig. 3.5 Rectangular flat shell element with 5 degrees of freedom at each node.

The flat element is simple to formulate, easy to describe by input data, easy to mix with other element types, and capable of rigid-body motion without strain. The stiffness matrix of the shell element will first be established in a local coordinate system. The element and the convention adapted for the local coordinate system are shown in Fig. 3.6.

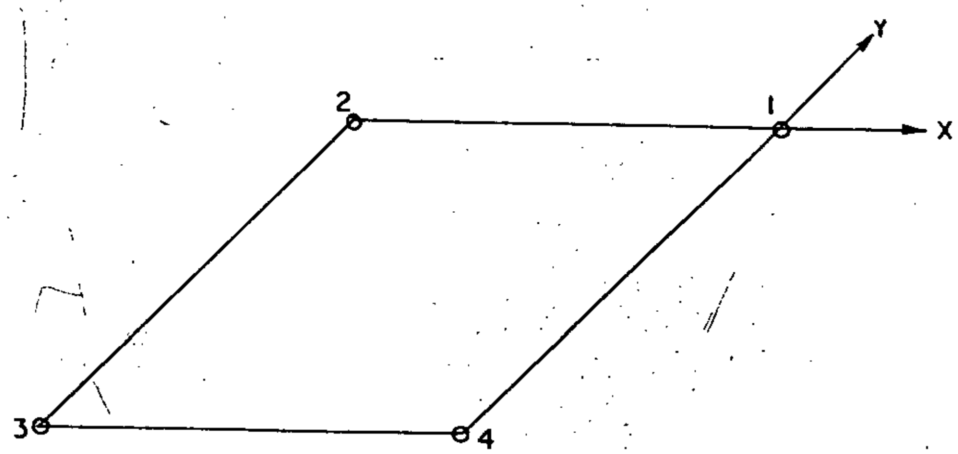

Fig. 3.6 Planar shell element in local coordinate system.

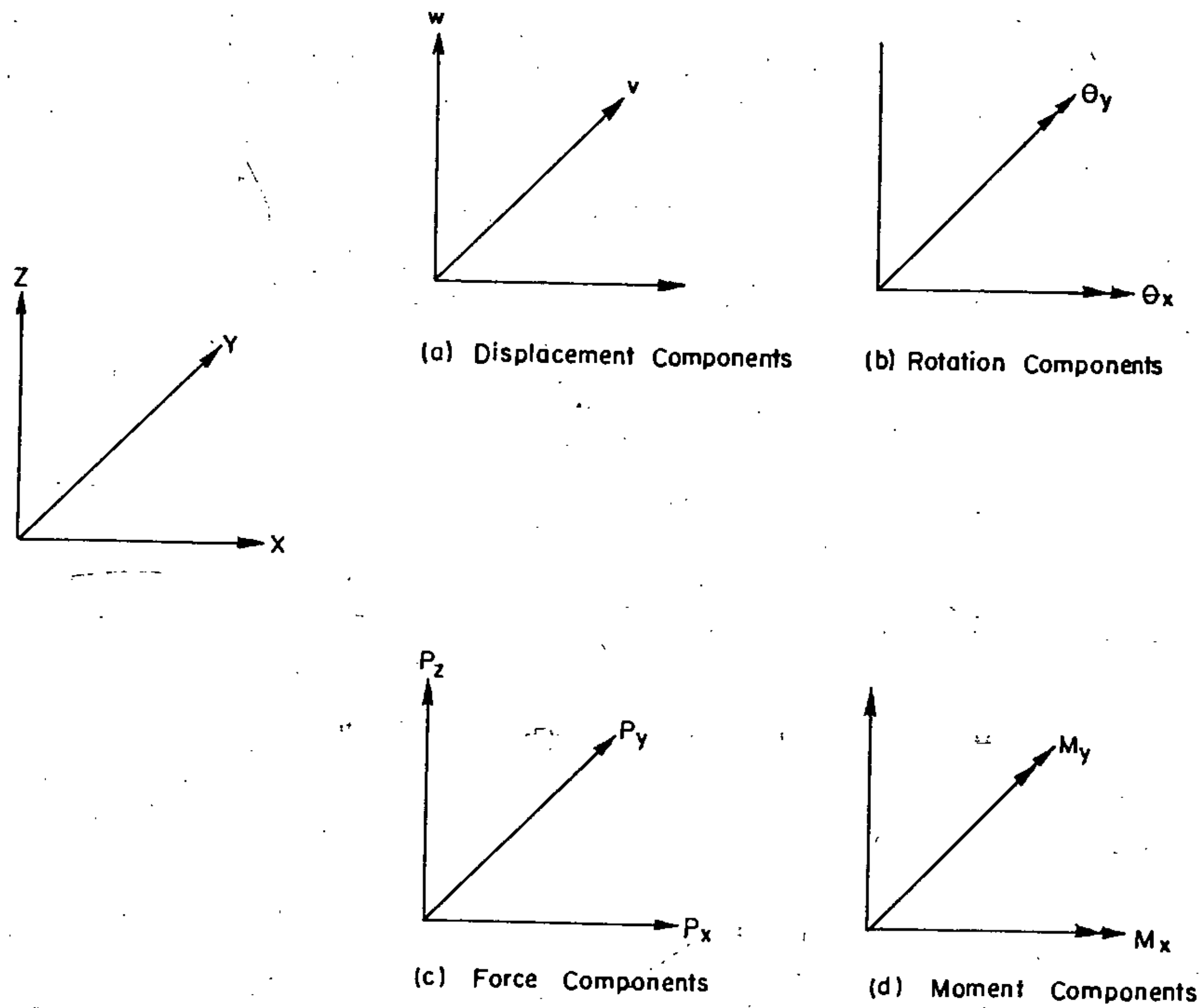

Fig. 3.7 Nodal displacement and force components.

Each of the four nodes is considered to have three displacement and two rotation components in space as nodal parameters. Thus there are 5 parameters related to each node. The parameters are denoted as shown in Fig. 3.7a and b. The corresponding stress resultants are denoted as shown in Fig. 3.7c and d. The quantities defined in Fig. 3.7 are assembled in the following vectors.

$$\{\underline{d}\}_i = \begin{bmatrix} u \\ v \\ w \\ \theta_x \\ \theta_y \end{bmatrix} \qquad \{\underline{F}\}_i = \begin{bmatrix} P_x \\ P_y \\ P_z \\ M_x \\ M_y \end{bmatrix} \qquad 3.13a,b$$

where index i denote node number i. The total vectors of nodal parameters and nodal stress resultants for the element are

$$\{\underline{d}\} = \begin{bmatrix} \underline{d}_1 \\ \underline{d}_2 \\ \underline{d}_3 \end{bmatrix} \qquad \{\underline{F}\} = \begin{bmatrix} \underline{F}_1 \\ \underline{F}_2 \\ \underline{F}_3 \end{bmatrix} \qquad 3.14a,b$$

The quantities $\underline{F}$ and $\underline{d}$ are related by the equations

$$\{\underline{F}\} = \left[\underline{K}\right] \left\{\underline{d}\right\} \qquad 3.15$$

where $\left[\underline{K}\right]$ is the stiffness matrix of the shell element referred to local coordinates.

Provided that the relative displacements, within the element are small, which is the usual assumption of linear structural theory, the in-plane action and the bending action are uncoupled.

The plane stress stiffness will be discussed in Art. 3.5.2, is chosen to describe the in-plane action and given in the form as shown in Eq. (3.16).

$$
\begin{bmatrix} \begin{bmatrix} P_x \\ P_y \end{bmatrix}_1 \\ \begin{bmatrix} P_x \\ P_y \end{bmatrix}_2 \\ \begin{bmatrix} P_x \\ P_y \end{bmatrix}_3 \\ \begin{bmatrix} P_x \\ P_y \end{bmatrix}_4 \end{bmatrix} = \begin{bmatrix} \underline{K}^P_{11} & \underline{K}^P_{12} & \underline{K}^P_{13} & \underline{K}^P_{14} \\ \underline{K}^P_{21} & \underline{K}^P_{22} & \underline{K}^P_{23} & \underline{K}^P_{24} \\ \underline{K}^P_{31} & \underline{K}^P_{32} & \underline{K}^P_{33} & \underline{K}^P_{34} \\ \underline{K}^P_{41} & \underline{K}^P_{42} & \underline{K}^P_{43} & \underline{K}^P_{44} \end{bmatrix} \begin{bmatrix} \begin{bmatrix} u \\ v \end{bmatrix}_1 \\ \begin{bmatrix} u \\ v \end{bmatrix}_2 \\ \begin{bmatrix} u \\ v \end{bmatrix}_3 \\ \begin{bmatrix} u \\ v \end{bmatrix}_4 \end{bmatrix} \qquad 3.16
$$

In Eq. 3.16 displacements and stress resultants related to node number 1 have been listed first, followed by the corresponding quantities for nodes number 2, 3 and 4. The superscript P has been added to denote plane stress.

The plate bending element with 12 degrees of freedom will discussed in Art. 3.5.3 is chosen for bending action. The stiffness matrix for this element is given in Eq. 3.17.

$$\begin{bmatrix} \begin{bmatrix} \underline{P}_z \\ M_x \\ M_y \end{bmatrix}_1 \\ \begin{bmatrix} P_z \\ M_x \\ M_y \end{bmatrix}_2 \\ \begin{bmatrix} P_z \\ M_x \\ M_y \end{bmatrix}_3 \\ \begin{bmatrix} P_z \\ M_x \\ M_y \end{bmatrix}_4 \end{bmatrix} = \begin{bmatrix} \underline{K}_{11}^B & \underline{K}_{12}^B & \underline{K}_{13}^B & \underline{K}_{14}^B \\ \underline{K}_{21}^B & \underline{K}_{22}^B & \underline{K}_{23}^B & \underline{K}_{24}^B \\ \underline{K}_{31}^B & \underline{K}_{32}^B & \underline{K}_{33}^B & \underline{K}_{34}^B \\ \underline{K}_{41}^B & \underline{K}_{42}^B & \underline{K}_{43}^B & \underline{K}_{44}^B \end{bmatrix} \begin{bmatrix} \begin{bmatrix} w \\ \theta_x \\ \theta_y \end{bmatrix}_1 \\ \begin{bmatrix} w \\ \theta_x \\ \theta_y \end{bmatrix}_2 \\ \begin{bmatrix} w \\ \theta_x \\ \theta_y \end{bmatrix}_3 \\ \begin{bmatrix} w \\ \theta_x \\ \theta_y \end{bmatrix}_4 \end{bmatrix} \qquad 3.17$$

In Eq. 3.17 the parameters have again been arranged in subvectors related to the nodes 1,2,3 and 4 respectively, and in each subvector the displacement normal to the plane of the plate has been placed first.

All necessary information for the formation of the stiffness matrix of Eq. 3.15 is now available. It only remains to place the submatrices of Eqs. 3.16 and 3.17 in the right positions in $[\underline{K}]$. The procedure is shown in Fig. 3.8 for the top four submatrices in $[\underline{K}]$. The remaining 8 submatrices are formed in the same manner.

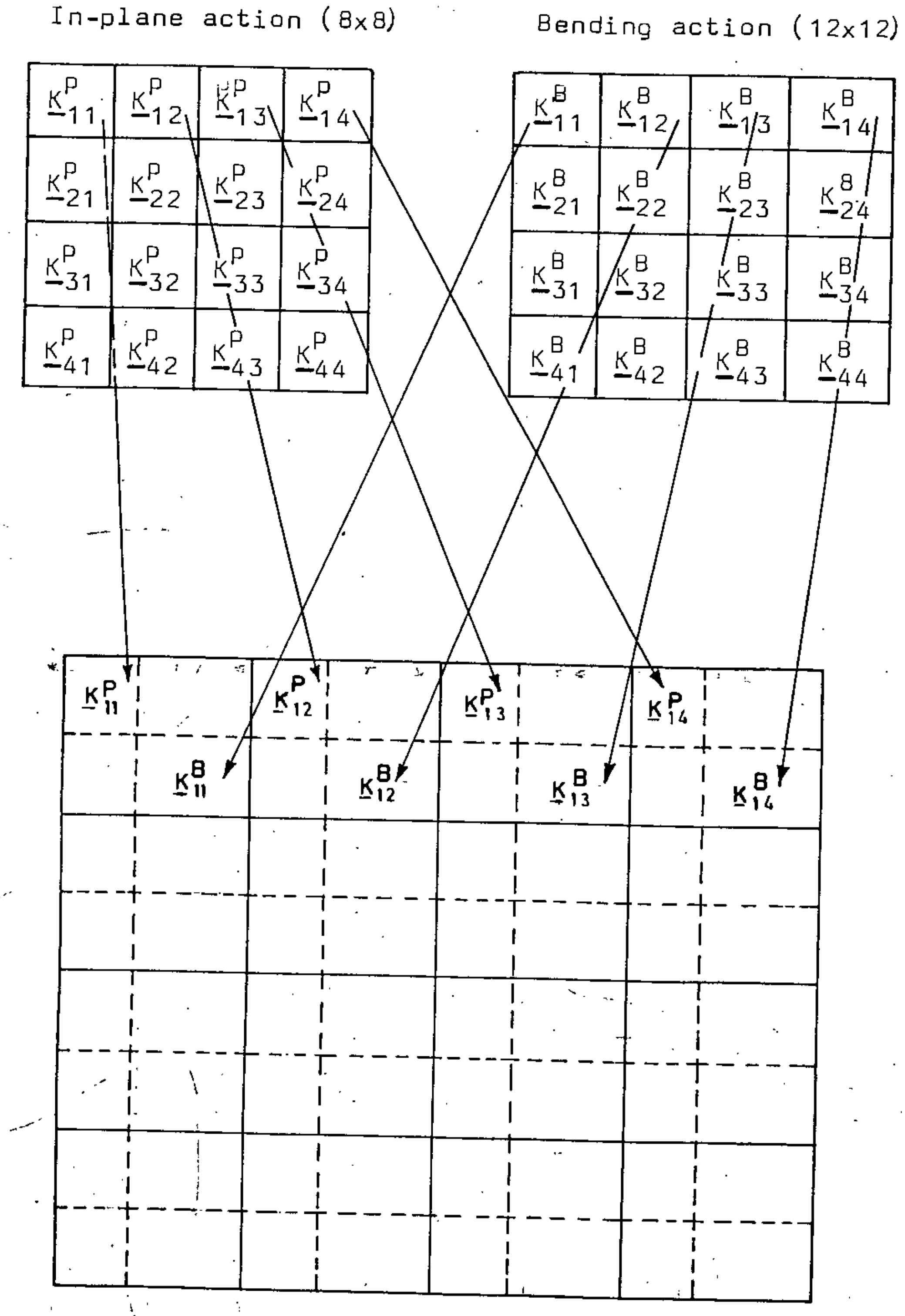

Fig. 3.8 Construction of the stiffness matrix for the shell element by use of stiffness matrices for plane stress and plate bending.

3.5.2 Plane Stress Element

Isoparametric quadratic plane elements are used to develop stiffness matrix for the in-plane action. Any standard text can provide the formulation required for developing the plane stress stiffness matrix. The author uses the formulation given by Bathe and Wilson[19].

3.5.3 Plate Bending Element

The finite element method is being applied extensively in plate bending problems, since it was first used by Adini and Clough[14] and Melosh[15]. In order to evaluate the stiffness matrix of the individual elements, the displacement patterns within the elements have to be assumed. The accuracy of the finite element procedure depends directly on the extent to which the assumed displacement functions are able to reproduce the actual distortions in the continuum. Clough and Tocher[20] have carried out a comparative study of the various displacement functions which have been suggested for use in plate bending problems. They studied 3 shapes suggested for rectangular elements and 4 shapes for triangular elements and from 280 different analyses of different plates, they concluded that 'two of the rectangular elements (M and ACM) and the compatible triangular element (HCT) provide very satisfactory analyses when used in the finite element analyses of plate bending. These two rectangular elements are somewhat more accurate than the triangular element, particularly when a coarse mesh is used and therefore are to be recommended for the analysis of any system in which the boundaries fit the rectangular co-ordinate area. Since floor slabs are usually composed of rectangular areas, it was decided to use rectangular elements.

The ACM displacement function is 12 term polynomial

$$W = a_1 + a_2 x + a_3 y + a_4 x^2 + a_5 xy + a_6 y^2 + a_7 x^3 + a_8 x^2 y + a_9 xy^2 + a_{10} y^3 + a_{11} xy^3 + a_{12} xy^3 \qquad 3.18$$

The element stiffness matrix derived from the above displacement function is shown in Appendix-A.

3.5.4 Beam Element

In the present analysis the beam is assumed to act compositely with the slab coupling it. So it will not be unjustified to take as much degrees of freedom in the beam node as in the slab nodal point. So the degrees of freedom and convention taken is shown in the Fig. 3.9 and 3.10.

It is to be noted that since the analyses are carried on the floor slab elements only and since the plane of slab can be any of the plane of Global coordinate plane there is no need for transforming slab element stiffness matrix from local to Global stiffness matrix. Also in general the beam elements are in orthogonal direction, so two types of beam elements are used, one in x-direction Fig. 3.9 and other in Y-direction Fig. 3.10.

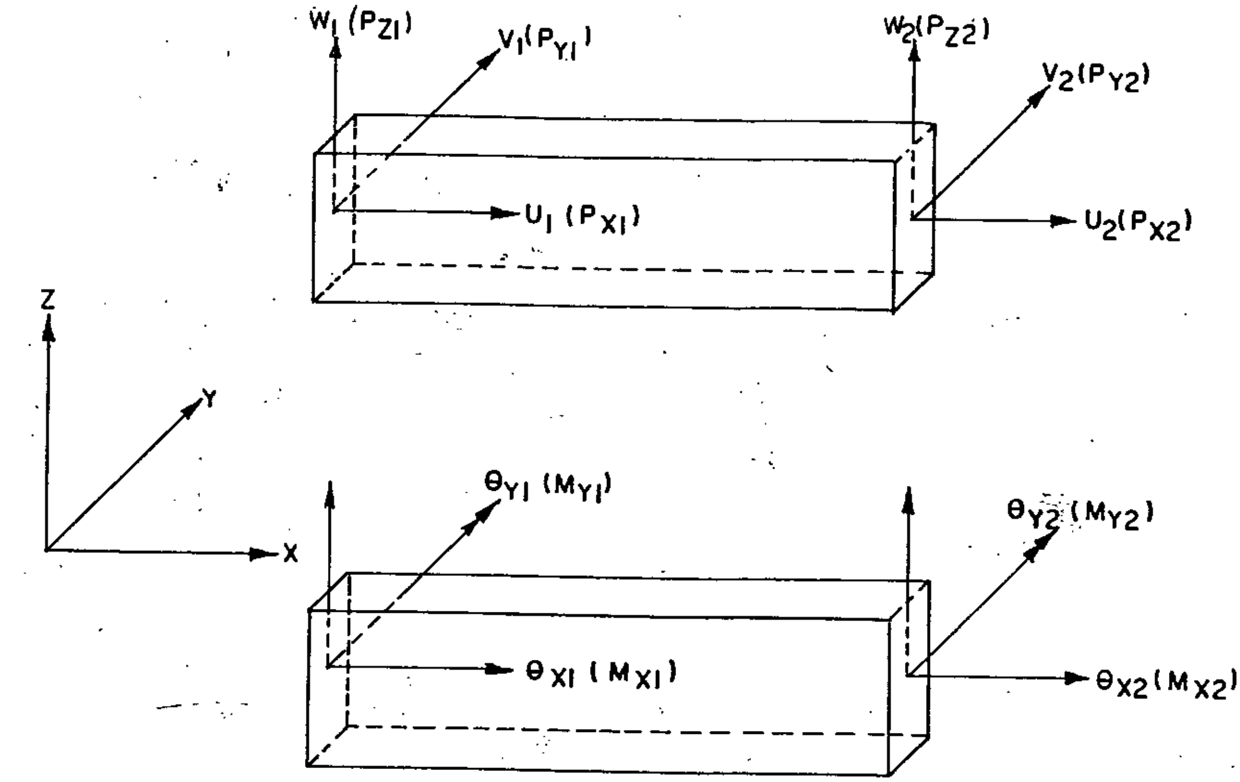

Fig. 3.9 Beam element in x-direction.

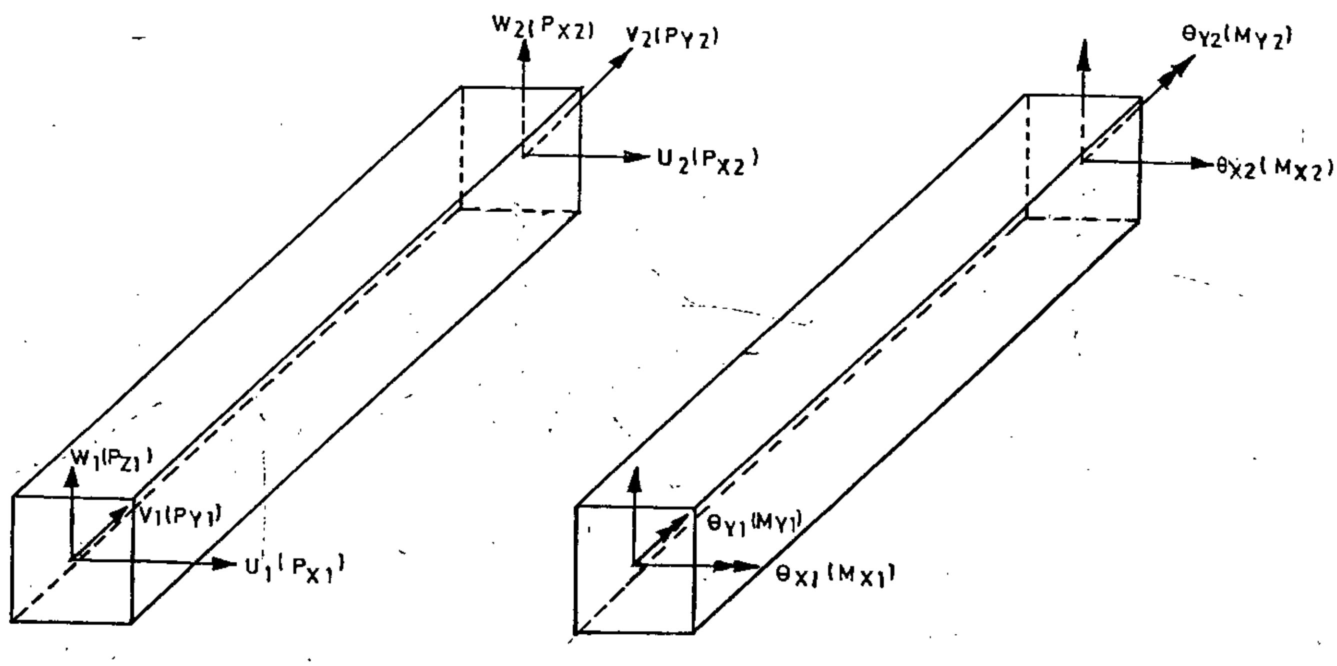

Fig. 3.10 Beam element Y-direction.

The element stiffness matrix with 5 degrees of freedom for both types of beam element are shown in Appendix-A.

3.5.5 Rigid Links (Composite Elements)

Lintel beam is assumed to act compositely with the slab. Usually the neutral surfaces of the plate and beam are not coincident. Therefore, to keep displacement compatibility between beam element and plate and to reduce the total number of nodes, beam stiffness matrix is developed for the degrees of freedom of the adjacent plates node connected with the beam. A standard preliminary treatment is to connect adjacent plate and beam nodes by rigid link, so that d.o.f of the beam are replaced by d.o.f of the plate. The usual assembly is then possible. The necessary transformation is now described.

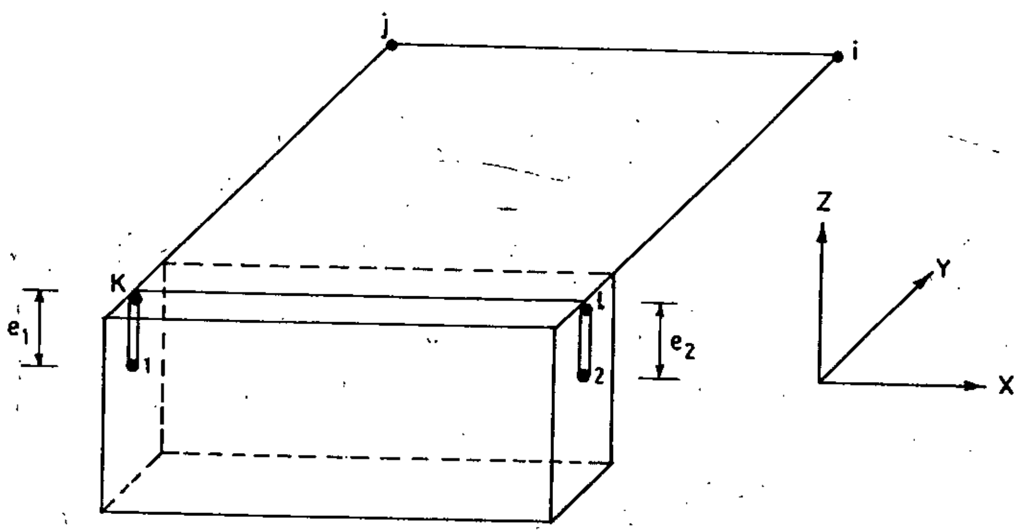

Fig. 3.11 Nodes 1 and 2 of a beam element are made slave to nodes k and ℓ by rigid links 1k and 2ℓ.

The beam element used has 10 d.o.f - 5 at node 1 and 5 at node 2. With reference to these d.o.f, element load and stiffness matrices are $\underline{r}'$ and k'. Similar d.o.f. are used at nodes k and ℓ of the rigid links 1k and 2ℓ. The "master" d.o.f. at node k and "slave" d.o.f at node 1 have the relation

$$\begin{Bmatrix} u_1 \\ v_1 \\ w_1 \\ \theta_{x1} \\ \theta_{y1} \end{Bmatrix} = \begin{bmatrix} \underline{\lambda}_1 \end{bmatrix} \begin{Bmatrix} u_k \\ v_k \\ w_k \\ \theta_{xk} \\ \theta_{yk} \end{Bmatrix}$$

where
$$\begin{bmatrix} \underline{\lambda}_1 \end{bmatrix} = \begin{bmatrix} 1 & 0 & 0 & 0 & -e_1 \\ 0 & 1 & 0 & c & 0 \\ 0 & 0 & 1 & 0 & 0 \\ 0 & 0 & 0 & 1 & 0 \\ 0 & 0 & 0 & 0 & 1 \end{bmatrix} \qquad 3.19$$

where e_1 = eccentricity between plate node and beams centroidal node. (+ve if plate neutral plane is above the beam neutral plane).

A similar expression is written for link 2ℓ by replacing subscripts 1 and k by 2 and ℓ . The transformed arrays $\{r\}$ and $\begin{bmatrix} \underline{k} \end{bmatrix}$ associated with d.o.f at nodes k and ℓ , are

$$\{\underline{r}\} = [\underline{T}]^T \{r'\}$$

$$\text{and} \quad [\underline{k}] = [\underline{T}]^T [\underline{k}'] [\underline{T}]$$

$$\text{where} \quad \underset{10\times10}{[\underline{T}]} = \begin{bmatrix} \underline{\lambda}_1 & \underline{0} \\ \underline{0} & \underline{\lambda}_2 \end{bmatrix} \qquad 3.20$$

3.5.6 Degrees of Freedom of the Floor Slab[6]

In general, each nodeal point in the flat shell has five degrees of freedom $u, v, w, \theta_x, \theta_y$. In the case of flat shell supported on walls and columns, stiffness values are necessary in the overall analysis of the structure for only those degrees of freedom which correspond to the unknown displacements of the walls and columns. For example, in Fig. 3.12, stiffness of nodes $A_1, A_2, A_3, A_4, A_5, A_6$ and B_1, B_2, B_3 will be sufficient in carrying out the overall analysis of

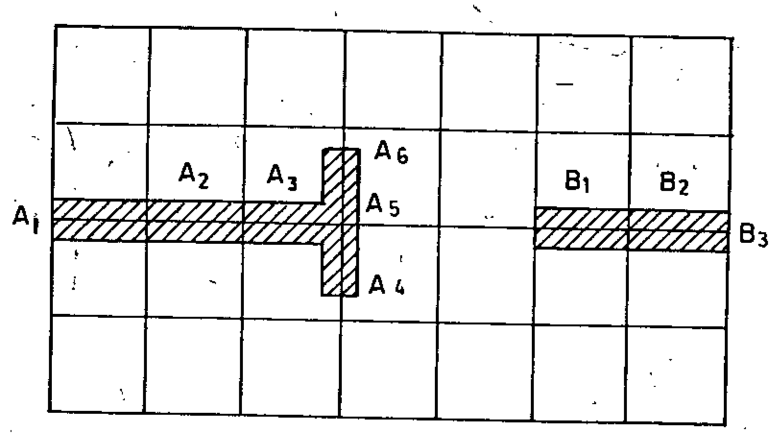

Fig. 3.12 Finite element idealization of floor slab.

the structure. Thus, it is not necessary to incorporate the full finite element stiffness matrix of the slab in the analysis of walls. Instead, stiffness values corresponding to only those nodes which are coupled to the walls will suffice.

In the analysis of walls, it is assumed that plane sections of the walls before bending remain plane after bending. This implies that in order to maintain full compatibility with the wall displacements, the displacements of the floor nodes directly connected to the walls (viz. $A_1, A_2, A_3, A_4, A_5, A_6, B_1, B_2$ B_3 in Fig. 3.12) must also be linearly related. Consequently, displacements for all the nodes connected to any particular wall may be referred to only one node (viz. displacements of B_1 and B_2 may be referred to the displacements of B_3). So the nodes in the floor slab may be classified into the following categories:-

i) nodes which are completely free to displace and hence no nodal forces produced.

ii) nodes which are rigidly connected to other nodes and hence their displacements bear a linear relationship with each other.

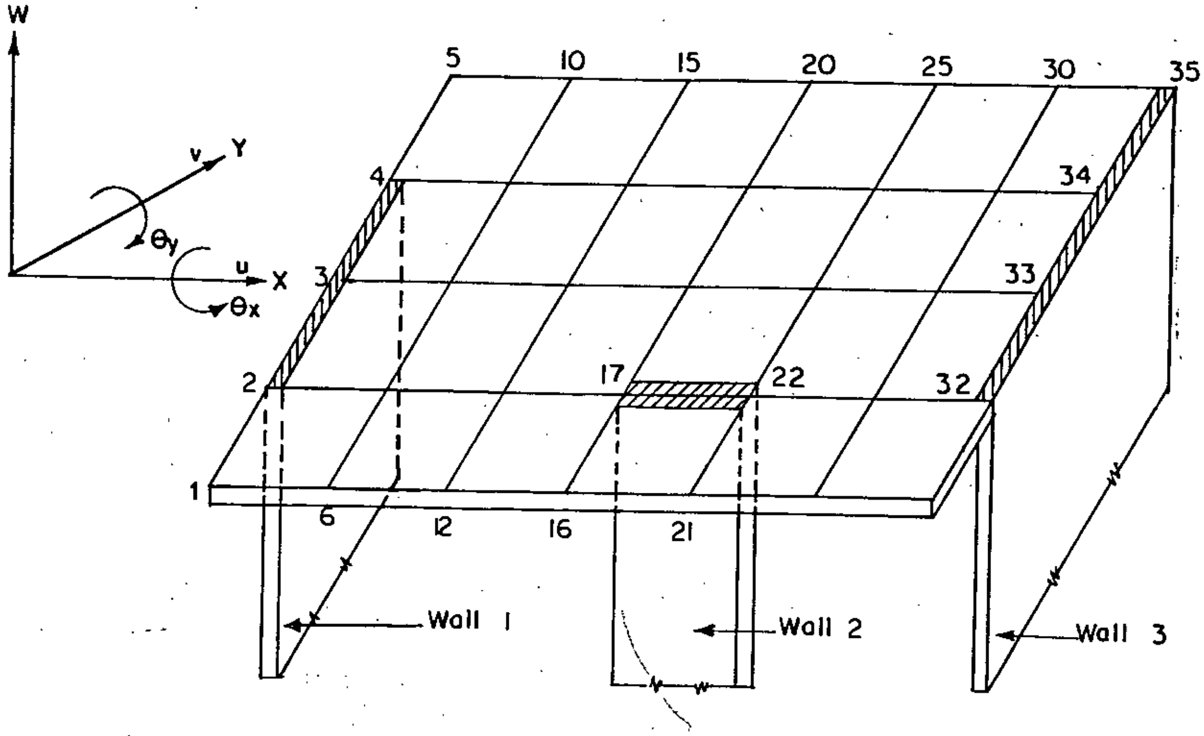

Fig. 3.13 Finite element idealization of floor slab.

In Fig. 3.13, nodes 2, 3, 4, 17, 22, 32, 33, 34 and 35 fall into the first category.

The displacements of all nodes lying on wall 1, node nos. 2, 3, 4, are linearly related to each other and these may be expressed in terms of the displacements of any of the 3 nodes. Taking node 3 as the reference node:

$$u_2 = u_3$$

$$v_2 = v_3, \text{ as we neglect the inplane rotation}$$

$$w_2 = w_3 - (y_3 - y_2)\ \theta_{x,3} + (x_3 - x_2)\,\theta_{y,3}$$

$$\theta_{x,2} = \theta_{x,3}$$

$$\theta_{y,2} = \theta_{y,3}$$

or $\quad \left[\delta_2\right] = \left[\tau_2\right]\ \left[\delta_3\right]$

and $u_4 = u_3$

$$v_4 = v_3$$

$$w_4 = w_3 - (y_3 - y_4)\,\theta_{x,4} + (x_3 - x_4)\,\theta_{y,3}$$

$$\theta_{x,4} = \theta_{x,3}$$

$$\theta_{y,4} = \theta_{y,3}$$

or $\left[\delta_4\right] = \left[\tau_4\right] \left[\delta_3\right]$

Similar equations may be written for the other walls. Although, in the analysis of the floor slab, the reference node may be selected arbitrarily, as long as it lies on the wall, these stiffnesses have to be transformed to correspond to the wall-centroids before they can be incorporated into the equivalent frame programme for the analysis of walls.

3.5.7 Condensation of the Stiffness Matrix[6]

Let $\left[\underline{K}\right] \{\underline{u}\} = \{\underline{p}\}$ 3.22

represent the nodal equilibrium equations for the finite element idealization of the floor.

$\underline{K}$ is the stiffness matrix assembled by the superposition of nodal stiffnesses, obtained from element stiffness matrices.

$\underline{u}$ is the displacement vector which refers to all the displacements.

and $\underline{p}$ is the load vector corresponding to these displacements.

The displacement $\underline{u}$ contains all the possible degrees of freedom of the discretized structure, 5 x (number of nodal points). Let this displacement vector be partitioned into three vectors:

i) $\underline{u}_1$ which refers to the displacementsof nodal points taken as reference points.

ii) $\underline{u}_2$ which refers to the displacements of the nodal points rigidly connected to the reference nodes in (i)

and iii) $\underline{u}_3$ which refers to the displacements of all other nodal points that are not on the walls (i.e, free nodes).

Let the load vector $\underline{P}$ be partitioned into vectors $\underline{P}_1$, $\underline{P}_2$ and $\underline{P}_3$ corresponding to the displacements, $\underline{u}_1$, $\underline{u}_2$ and $\underline{u}_3$ respectively.

$$\text{So} \quad \left\{\underline{u}\right\} = \begin{bmatrix} \underline{u}_1 \\ \underline{u}_2 \\ \underline{u}_3 \end{bmatrix} \quad \text{and} \quad \left\{\underline{P}\right\} = \begin{bmatrix} \underline{P}_1 \\ \underline{P}_2 \\ \underline{P}_3 \end{bmatrix} \qquad 3.23$$

$$\text{and} \quad \left[\underline{K}\right] \begin{bmatrix} \underline{u}_1 \\ \underline{u}_2 \\ \underline{u}_3 \end{bmatrix} = \begin{bmatrix} \underline{P}_1 \\ \underline{P}_2 \\ \underline{P}_3 \end{bmatrix} \qquad 3.24$$

The stiffness matrix $\underline{K}$ may be partitioned to givethe sub-matrices corresponding to the three groups of displacements:

$$\begin{bmatrix} \underline{K}_{11} & \underline{K}_{12} & \underline{K}_{13} \\ \underline{K}_{21} & \underline{K}_{22} & \underline{K}_{23} \\ \underline{K}_{31} & \underline{K}_{32} & \underline{K}_{33} \end{bmatrix} \begin{bmatrix} \underline{u}_1 \\ \underline{u}_2 \\ \underline{u}_3 \end{bmatrix} = \begin{bmatrix} \underline{P}_1 \\ \underline{P}_2 \\ \underline{P}_3 \end{bmatrix} \qquad 3.25$$

Since the displacement vectors $\underline{u}_1$ and $\underline{u}_2$ are related to each other linearly,

$$\left\{\underline{u}_2\right\} = \left[\underline{T}_1\right] \left\{\underline{u}_1\right\} \qquad 3.26$$

where $\underline{T}_1$ is a linear transformation matrix.

For example, in the plate shown in Fig. 3.13, taking nodes 3, 17 and 34 as the reference nodes for walls 1,2, and 3 respectively.

Displacements of nodes 3,17, and 34	Form displacement vector $\underline{u}_1$
Displacements of nodes 2,4,22,32, 33, and 35	Form the displacement vector $\underline{u}_2$
Displacements of-nodes the remaining nodes	Form the displacement vector $\underline{u}_3$

The transformation matrix, relating $\underline{u}_2$ and $\underline{u}_3$, may be written by inspection of the deflected shape. Keeping in view that, as plane sections of the wall before bending are assumed to remain plane after bending, all the nodes connected to a particular wall must also lie on the same plane after bending. Hence, the slopes at the nodes must be the same and the vertical deflections must be linearly related.

The transformation matrix T_1 may from Eqs. 3.21.

$$
\begin{bmatrix} u_2 \\ v_2 \\ w_2 \\ {}_{x,2} \\ {}_{y,2} \\ \hline u_4 \\ v_4 \\ w_4 \\ {}_{x,4} \\ \hline u_{22} \\ v_{22} \\ w_{22} \\ \theta_{x,22} \\ \theta_{y,22} \\ \hline \vdots \\ \hline u_{35} \\ v_{35} \\ w_{35} \\ \theta_{x,35} \\ \theta_{x,35} \\ \theta_{y,35} \end{bmatrix}
=
\begin{bmatrix} \underline{\lambda}_1 & \underline{0} & \underline{0} \\ \underline{\lambda}_2 & \underline{0} & \underline{0} \\ \underline{0} & \underline{\lambda}_3 & \underline{0} \\ \underline{0} & \underline{0} & \underline{\lambda}_4 \\ \underline{0} & \underline{0} & \underline{\lambda}_5 \\ \underline{0} & \underline{0} & \underline{\lambda}_6 \end{bmatrix}
\begin{bmatrix} \underline{u}_3 \\ v_3 \\ w_3 \\ \theta_{x,3} \\ \theta_{y.3} \\ \hline u_{17} \\ v_{17} \\ w_{17} \\ \theta_{x,17} \\ \theta_{y,17} \\ \hline u_{34} \\ v_{34} \\ \theta_{x,34} \\ \theta_{y,34} \end{bmatrix}
$$

$$\text{or} \quad \{\underline{u}_2\} = \left[\underline{T}_1\right] \{\underline{u}_1\} \qquad 3.27$$

where,

$$\underline{\lambda}_1 = \begin{bmatrix} 1 & 0 & 0 & 0 & 0 \\ 0 & 1 & 0 & 0 & 0 \\ 0 & 0 & 1 & -(y_3-y_2) & (x_3-x_2) \\ 0 & 0 & 0 & 1 & 0 \\ 0 & 0 & 0 & 0 & 1 \end{bmatrix}$$

$$\underline{\lambda}_2 = \begin{bmatrix} 1 & 0 & 0 & 0 & 0 \\ 0 & 1 & 0 & 0 & 0 \\ 0 & 0 & 1 & -(y_3-y_4) & (x_3-x_4) \\ 0 & 0 & 0 & 1 & 0 \\ 0 & 0 & 0 & 0 & 1 \end{bmatrix}$$

$$\underline{\lambda}_3 = \begin{bmatrix} 1 & 0 & 0 & 0 & 0 \\ 0 & 1 & 0 & 0 & 0 \\ 0 & 0 & 1 & -(y_{17}-y_{22}) & (x_{17}-x_{22}) \\ 0 & 0 & 0 & 1 & 0 \\ 0 & 0 & 0 & 0 & 1 \end{bmatrix}$$

Similarly $\underline{\lambda}_4$, $\underline{\lambda}_5$, $\underline{\lambda}_6$ can be derived.

Therefore,

$$\{\underline{u}\} = \begin{bmatrix} \underline{u}_1 \\ \underline{u}_2 \\ \underline{u}_3 \end{bmatrix} = \begin{bmatrix} \underline{u}_1 \\ \underline{T}_1 u_1 \\ \underline{u}_3 \end{bmatrix} = \begin{bmatrix} \underline{I} & \underline{0} \\ \underline{T}_1 & \underline{0} \\ \underline{0} & \underline{I} \end{bmatrix} \begin{bmatrix} \underline{u}_1 \\ \underline{u}_3 \end{bmatrix} = \begin{bmatrix} \underline{T}_2 \end{bmatrix} \begin{bmatrix} \underline{u}_1 \\ \underline{u}_3 \end{bmatrix} \qquad 3.28$$

where

$$\left[\underline{T}_2\right] = \begin{bmatrix} \underline{I} & 0 \\ \underline{T}_1 & \underline{0} \\ \underline{0} & \underline{I} \end{bmatrix} \qquad 3.29$$

and $\underline{I}$ represents unit matrices, of such order as to make themconforming for multiplication with the appropriate vectors.

Applying the contragredient relationship that exist between the forces and displacements to Eq. 3.28.

$$\begin{bmatrix} \underline{P}_1 \\ \underline{P}_3 \end{bmatrix} = \left[\underline{T}_2^*\right] \begin{bmatrix} \underline{P}_1 \\ \underline{P}_2 \\ \underline{P}_3 \end{bmatrix} \qquad 3.30$$

Eq. 3.24 may now be rewritten as

$$\left[\underline{K}\right] \left[\underline{T}_2\right] \begin{bmatrix} \underline{u}_1 \\ \underline{u}_3 \end{bmatrix} = \begin{bmatrix} \underline{P}_1 \\ \underline{P}_2 \\ \underline{P}_3 \end{bmatrix} \qquad 3.31$$

Premultiplying both sides by $\underline{T}_2^*$,

$$\left[\underline{T}_2^* \quad \underline{K} \quad \underline{T}_2\right] \begin{bmatrix} \underline{u}_1 \\ \underline{u}_3 \end{bmatrix} = \left[\underline{T}_2^*\right] \begin{bmatrix} \underline{P}_1 \\ \underline{P}_2 \\ \underline{P}_3 \end{bmatrix} = \begin{bmatrix} \underline{P}_1 \\ \underline{P}_3 \end{bmatrix} \qquad 3.32$$

Writing $\underline{K}$ in its partitioned form, as inneq. (3.25) and substituting the values of $\underline{T}_2$ and $\underline{T}_2^*$,

$$\begin{bmatrix} \underline{I} & \underline{T}_1^* & \underline{0} \\ \underline{0} & \underline{0} & \underline{I} \end{bmatrix} \begin{bmatrix} \underline{K}_{11} & \underline{K}_{12} & \underline{K}_{13} \\ \underline{K}_{21} & \underline{K}_{22} & \underline{K}_{23} \\ \underline{K}_{31} & \underline{K}_{32} & \underline{K}_{33} \end{bmatrix} \begin{bmatrix} \underline{I} & \underline{0} \\ \underline{T}_1 & \underline{0} \\ \underline{0} & \underline{I} \end{bmatrix} \begin{bmatrix} \underline{u}_1 \\ \underline{u}_3 \end{bmatrix} = \begin{bmatrix} \underline{P}_1 \\ \underline{P}_3 \end{bmatrix} \qquad 3.33$$

Carrying out the matrix multiplication, and noting that, since the displacement vector u_3 refers to nodal displacements which do not have any external restraint imposed on them, the corresponding load vector P_3 must be zero,

$$\begin{bmatrix} (\underline{K}_{11}+\underline{T}_1^*\underline{K}_{21}+\underline{K}_{12}\underline{T}_1+\underline{T}_1^*\underline{K}_{22}\underline{T}_1) & (\underline{K}_{13}+\underline{T}_1^*\underline{K}_{23}) \\ \underline{K}_{31}+\underline{K}_{32}\underline{T}_1 & \underline{K}_{33} \end{bmatrix} \begin{bmatrix} \underline{u}_1 \\ \underline{u}_3 \end{bmatrix} = \begin{bmatrix} \underline{P}_1 \\ \underline{0} \end{bmatrix} \qquad 3.34$$

Eliminating $\underline{u}_3$ from Eq. 3.34,

$$\left[(\underline{K}_{11} + \underline{T}_1^*\underline{K}_{21} + \underline{K}_{12}\underline{T}_1 + \underline{T}_1^*\underline{K}_{22}\underline{T}_1) - (\underline{K}_{13} + \underline{T}_1^*\underline{K}_{23}) \times (\underline{K}_{33}^{-1})(\underline{K}_{31} + \underline{K}_{32}\underline{T}_1)\right] \left[\underline{u}_1\right] = \left[\underline{P}_1\right]$$

or

$$\left[\underline{K}_c\right]\left[\underline{u}_1\right] = \left[\underline{P}_1\right] \qquad 3.35$$

where :

$$\left[\underline{K}_c\right] = \left[(\underline{K}_{11}+\underline{T}_1^{*}\cdot\underline{K}_{21} + \underline{K}_{12}\,\underline{T}_1 + \underline{T}_1^{*}\cdot\underline{K}_{22}\,\underline{T}_1) - (\underline{K}_{13} + \underline{T}_1^{*}\cdot\underline{K}_{23})(\underline{K}_{33}^{-1})(\underline{K}_{31}+\underline{K}_{32}\underline{T}_1)\right] \quad 3.36$$

is the condensed stiffness matrix of the plate, the displacements being referred to one node point for each wall. If the reference node for a wall does not correspond to the centroid of the wall the matrix $\underline{K}_c$ may be transformed by using a transformation matrix defining the location of the centroid of the wall with-respect to the reference node.

3.6 Computer Programme

Fig. 3.14 shows a flow diagram of the computer programme developed for the evaluation of the floor slab stiffnesses. This programme differs from other finite element programme in that instead of solving for externally applied displacements by means of matrix condensation.

The basic floor data, such as the number of elements, number of nodal points are read first. The data describing the element properties may be generated partly and partly read in it. From the element property data the elements are taken as flat shell element or beam element. Explicit expressions for the stiffness matrices of the elements have been calculated and these are used in evaluating the stiffness matrix. It is worth noting that an orthotropic flat shell element may be included with very little modification in the data entry.

The concept of bandwidth is used in storing and operating on the assembled stiffness matrix. By careful numbering of nodes, the band width may be kept a minimum.

Any external restraint, e.g. those imposed due to continuity of the plate or fixity of the plate, may be applied before condensing the stiffness matrix.

The condensation of the stiffness matrix involves the solution of eq. 3.35. The matrix T_1 is usually large, but has few non-zero elements, consisting only of submatrices λ_i's which one of the form shown in eq. 3.21. In the programme only these τ_i's are formed with a consequent saving in the storage required.

A listing of the computer programme together with an explanation of details and form of data input is given in Appendix-B.

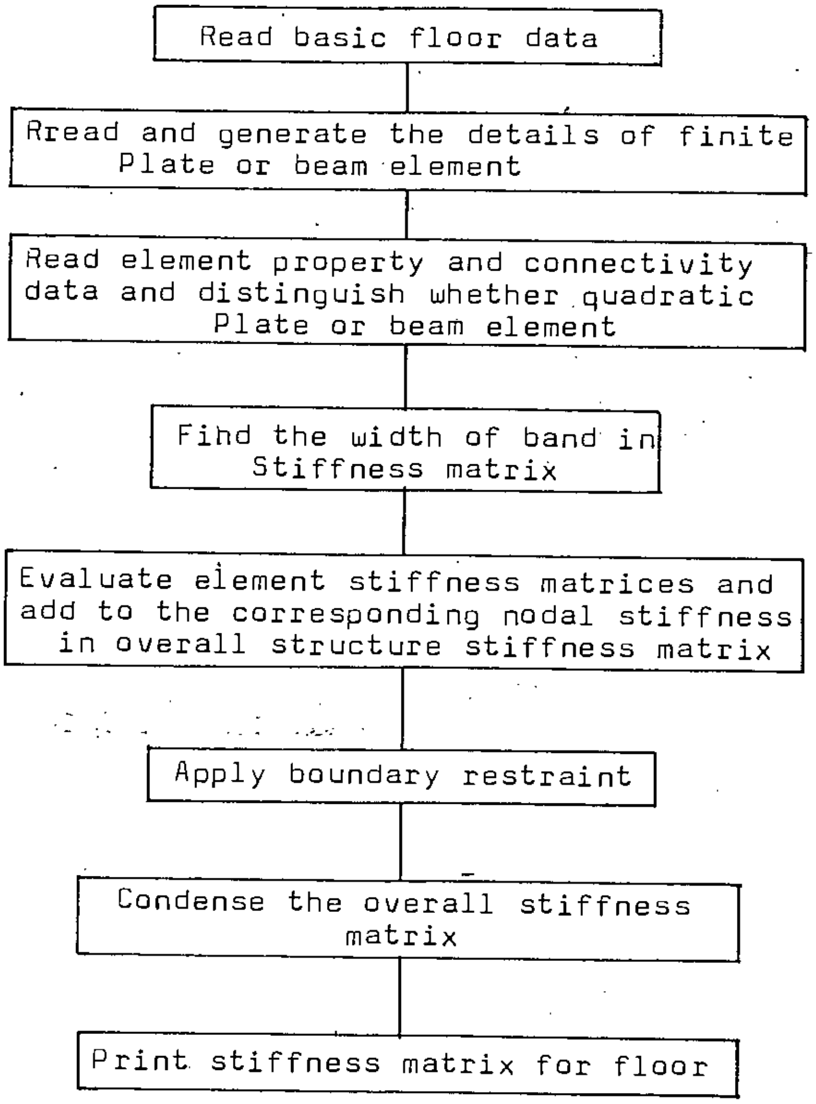

Fig. 3.14 Flow diagram of the programme for the finite element analysis of floor slab stiffness.

CHAPTER 4

RESULTS AND DISCUSSIONS

4.1 Introduction

In order to study the composite coupling action of beam and slab connecting a pair of shear walls, the plate in Fig. 4.1(a) was analysed. The dimension X is length, Y is width of the slab, L is the clear opening between walls, Z-is the flange width of walls (in case of T-shaped, I-shaped walls), W_1 and W_2 are the lengths of two walls. In order to study the effect of different wall configuration, in-line plane walls, T-shaped walls, I-shaped walls and one T-shaped and another plane walls were taken in the study. The different wall configurations used are shown in Fig. 4.1.

Line B_1 B_2 indicates the position of beam connecting the two walls. In order to study the effect of beam stiffness on the effective width, different sizes of beam are considered in the study.

Since the rotational stiffness K of the composite beam is affected directly by the change in the linear distance between wall centres as the wall configuration is changed, the results for the stiffness factor do not give a clear picture of the actual influence of the wall configuration and beam size on the effective coupling slab width. Hence, in order to assess more succinctly the influence of wall configuration and beam size, reference is made only to the results obtained for the effective width to the slab width ratio, Y_e/Y.

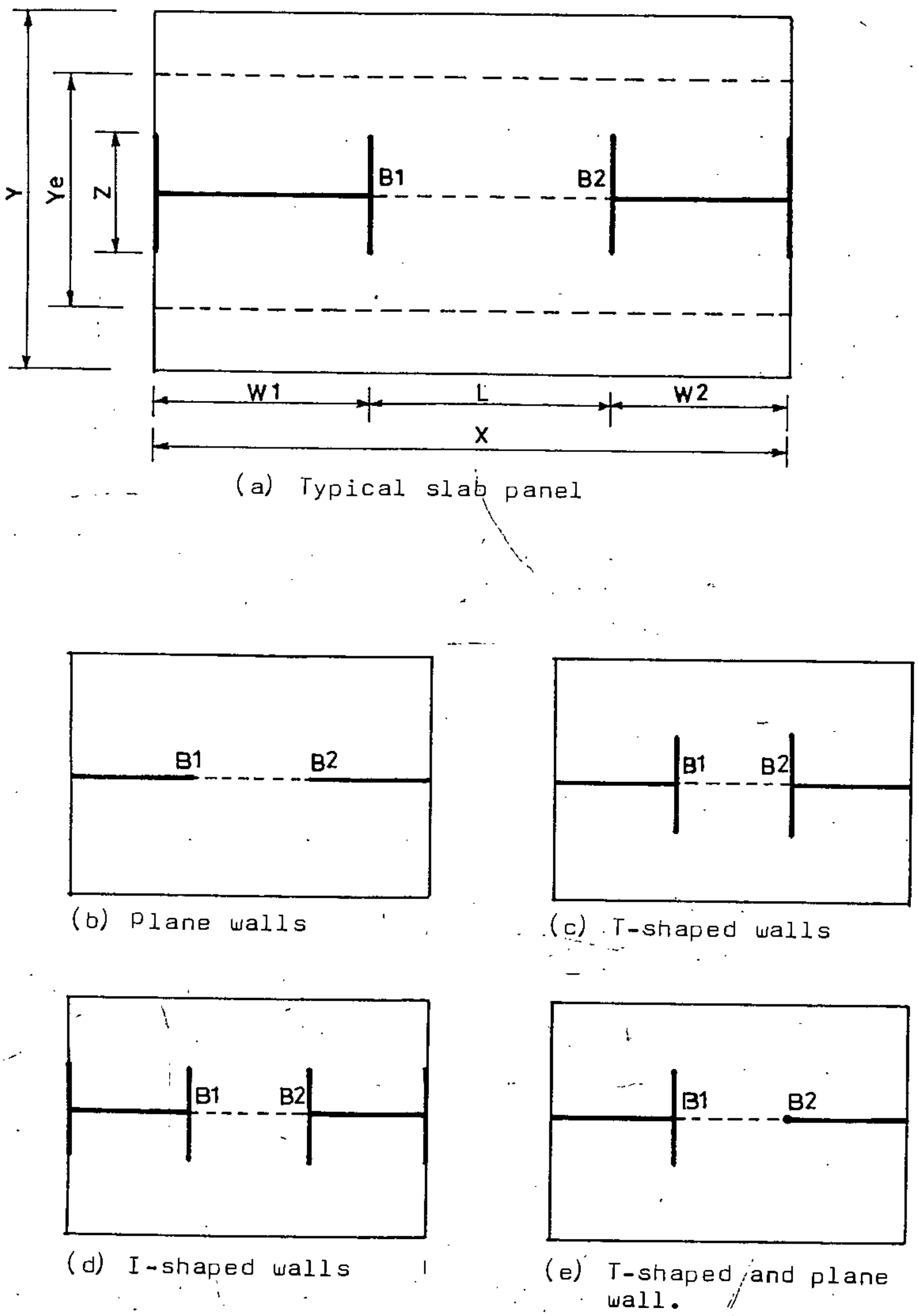

Fig. 4.1 Different wall configurations.

4.2 Coupling Action of Slab (without beams)

There are several papers on the coupling action of slab in shear wall structures. Figs. 4.2 and 4.3 have been prepared to compare the results of this study with those available in the papers.

4.2.1 Plane Shear Walls

The plate shown in Fig. 4.1(b) without connecting beam B_1 B_2 is analysed. Keeping L, X constant and varying Y only, the variation of Y_e/Y with the ratio of wall opening to slab width (L/Y) is studied and Y_e/Y vs. L/Y curve is shown in Fig. 4.2. From the design curves given by Coull and Wong(12) the values of Y_e/Y for various L/Y ratios are plotted on the same Fig. 4.2 and these give close agreement with the observed results. Similar results are observed from the design curves by Tso and Mahmood(22).

4.2.2 T-shaped Shear Walls

The plate shown in Fig. 4.1(c) without beam B_1 B_2 is analyzed. Keeping L, X and Z constant and varying Y only the variation of Y_e/Y with the ratio of wall opening to slab width L/Y is studied and shown in Fig. 4.3 as a firm line. From the design curves given by Coull and Wong(12), the values of Y_e/Y for different L/Y ratios are plotted in the same figure. For the higher range of L/Y ratio, these give close agreement but at the lower value of L/Y these give some deviation (e.g. 3.7% higher for $L/Y = 0.375$) from the observed results.

4.3 Coupling Action of Slab and Beam

To demonstrate the effect and influence of beam flexibility on the effective flange width of the composite coupling beam various plates shown in Fig. 4.1 were analyzed and the results are shown from Fig. 4.4 to Fig. 4.13. Only one paper has so far been published on this topic, viz. by Coull and Wong(13). The paper considers only planar shear walls with connecting beams. On the concluding remarks they stated that the influence of the coupling action is significant only when the beam is relatively flexible. That remark can also be made from the study done here.

4.3.1 Plane Wall Configurations

It has been shown by Coull and Wong(12) that in walls coupled by slabs alone, the effects of dissimilar wall lengths may be disregarded, provided that the length of smaller wall is greater than about half the length of opening between walls. This will be true in almost all practical situations. In order to verify whether these above conclusion is valid for slabs with beams also, the variation of Y_e/Y with the ratio of one wall length to another wall length W_2/W_1 for different beam depth is studied and the result is shown in Fig. 4.4. for three ratios of W_2/W_1 - 0.5, 0.25 and 1.0. The trends of the results for the three cases are similar and the curves for each beam size are almost coincident. So the effect of dissimilar wall length may be disregarded whether beam is present or absent.

Effect of Different Beam Size

The variation of Y_e/Y with the ratio of beam depth to slab thickness d/t is shown in Fig. 4.4 for different ratios of wall opening to slab width. The trends of the results for the two cases are different but both the cases show that with the increase in L/Y ratio, Y_e/Y increases, rapidly for $d/t = 2$ (e.g. increasing L/Y ratio from 0.4 to 0.7, the value of Y_e/Y changed from 0.33 to 0.51 for W_2/W_1 - 0.5) and slowly for $d/t = 6$ (e.g. increasing L/Y ratio from 0.4 to 0.7, the value of Y_e/Y changed from 0.15 to 0.215). Fig. 4.10 shows the variation of Y_e/Y with different d/t ratios for two ratios of L/Y - 0.75 and 0.375. Here both the curves show that increase in beam depth decreases the Y_e/Y ratio, rapidly within the range to $2 < d/t < 5$. Thus it can concluded that beam reduces the influence of slab in the coupling action in coupled shear wall system.

Effect of Wall Opening Width

In the Fig. 4.4, Y_e/Y vs. L/Y is plotted for two values of d/t - 2 and 6. For both the values of d/t, Y_e/Y increases with the increase of L/Y.

From Fig. 4.4 it can be concluded that with increase in opening size, coupling action of the connecting slab increases.

For the increase in L/Y ratio 0.4 to 0.7, the increase in Y_e is 18% of slab width and 7% of slab width for d/t = 2 and d/t = 6 respectively.

4.3.2 T-section Walls

Flanged shear walls occur frequently in cross-wall structures as a result of making the corridor or facade longitudinal walls of similar construction to the cross-walls to satisfy the need for additional load bearing area or longitudinal stiffness, or simply for convenience in construction.

Effect of Flanges

Let us consider the pair of identical T-shaped walls shown in Fig. 4.1(c) which are symmetrical with respect to the panel centre lines. Previous study showed that the effects of dissimilar wall lengths may be disregarded. Thus, although the present study is confined to a study of composite beams coupling equal walls which rotate equally under the action of lateral forces, it may be anticipated for design purposes that the results will apply with sufficient accuracy to most practical situations.

A finite element analysis enabled a series of curves to be produced showing the variation of the effective width ratio Y_e/Y as a function of the wall opening ratio L/Y for various flange width ratios Z/L for the two d/t ratios of 2 and 6. These are shown in Fig. 4.5 , Fig. 4.6 and Fig. 4.7 for three L/X ratios of 0.15, 0.333 and 0.5. For d/t = 2, the effect of flange is prominent. The Y_e/Y ratios are obtained for Z/L ratio of 1.0, 0.75, 0.5 and 0.0. The trends of the results for the four cases are similar, the effective width increase with the increase in flange length. As an example, for increase in Z/L from 0.5 to 0.75, the increase in Y_e is from 62% to 70% of slab width for L/Y = 0.5. Approximately similar amount of increase is observed for different L/Y ratio.

For d/t = 6, the effect of flange is not so much prominent. In the above example, for increase in Z/L from 0.5 to 0.75, the increase in Y_e is from 28% to 28.6% of slab width. From the curves it is observed that for d/t = 6, flange does not affect much in the lower value of L/Y ratio but it is significant for higher L/Y ratio.

To investigate the effect of slab length, i.e slab length on the Y_e/Y, Fig. 4.5, 4.6 and 4.7 shows the variation of effective width Y_e/Y with L/X ratio. And it is found that for both the d/t ratio - 2 and 6 with the increase in L/X ratio Y_e/Y increases but the amount of increase is quite a small value. As an example, Y_e/Y for L/Y = 0.6, and L/X = 0.15 is .855

for $Z/L = 1$ and for the same case but with $L/X = 0.333$, $Y_e/Y =$ 0.91. Thus, the effect of slab length on the coupling action may be disregarded.

To demonstrate the effect of beam size on coupling action of T-section walls, Y_e/Y as a function d/t is shown in Fig. 4.12 for two r-tios of L/Y - 0.75 and 0.375. Here, as in the case of plane wall configuration, both the curves show that increase in beam depth decreases the Y_e/Y ratio, rapidly in the range $2 < d/t < 6$.

4.3.3 I-section Walls

Figure 4.1(d) shows a configuration with flanges at the interior ends as well as flanges at the exterior ends of the cross walls.

Effect of Flanges

In Fig. 4.9 Y_e/Y is shown as a function of the ratio of opening distance to slab width for three ratios of Z/L - 0.75, 0.5, and 1.0. The results show the same trends and values as in T-section walls with same flange length.

Figure 4.13 demonstrates the effect of beam sizes on effective slab width; this also gives the same trends and values for the T-section walls. Thus, the effect of exterior flange can be disregarded.

4.3.4 Plane Walls and T-shaped Flanged Walls

As before curves have been produced Fig. 4.8 showing the variation of Y_e/Y as a function L/Y for various ratios of Z/L. The trends of the results are similar as in the T-shaped walls but value is less.

To demonstrate the effect on beam sizes on an effective slab width, Fig. 4.11 is drawn. This figure also gives the same trends as in other configurations. Here as in other cases increases in beam depth decreases the Y_e/Y ratio, rapidly in the range $2 < d/t < 5$.

4.4 Effect of Shear Deformation of the Beam

The design curves presented are obtained neglecting shear deformation in the connecting beam.

To demonstrate the effect of shear deformation of the connecting beam on the effective width calculation, Y_e/Y vs. d/t are plotted in the Figs. 4.10 to 4.13 for various wall configuration considering shear deformation in the beams. And it is found that consideration of shear deformation decreases the effective width of the slab by less than 5% of the slab width for the extreme case considered (e.g. in the Fig. 4.10, for $L/Y = 0.75$ and for $d/t = 7.0$, consideration shear deformation decreases the value of Y_e/Y from 0.22 to 0.17).

4.5 Discussions

From the results it is observed that the most significant parameters that affect the coupling action is the wall opening distance. For all the cases studied, it is found that with the increase in wall opening length, the coupling action provided by the slab becomes more and more significant. This agrees with the empirical conclusions based on determination of effective width by assigning angle of dispersion Fig. 2.1.

It is also observed that length of the slab has negligible effect on the coupling action. Also dissimilar wall lengths do not have any significant effect on the coupling action. These can be explained by the fact that the coupling action is influenced by the property of the opening zone only.

From the observation of results for a system where one T-section wall is coupled with a planar wall, it is found that the effective width of slab is more than that when both the walls are planar and less than that when both the walls are of T-section. This is due to the action of walls flange in distributing the curvature farther along the slab width. Thus it is possible that the use of beam can be ommited when T-shaped walls are used.

Finally, the most significant observation is that the use of beam decreases the coupling action of slab. viz. in a coupled I-section walls, as d/t increase for 1.0 to 6.0, the value of Y_e/Y is found to be reduced from 0.7 to 0.18 for $L/Y = 0.375$.

The results obtained are neglecting shear deformation in the connecting beam and consideration of shear deformation in the connecting beam reduces the effective width of slab but the reduction is by less than 5% of the slab width for the extreme case considered.

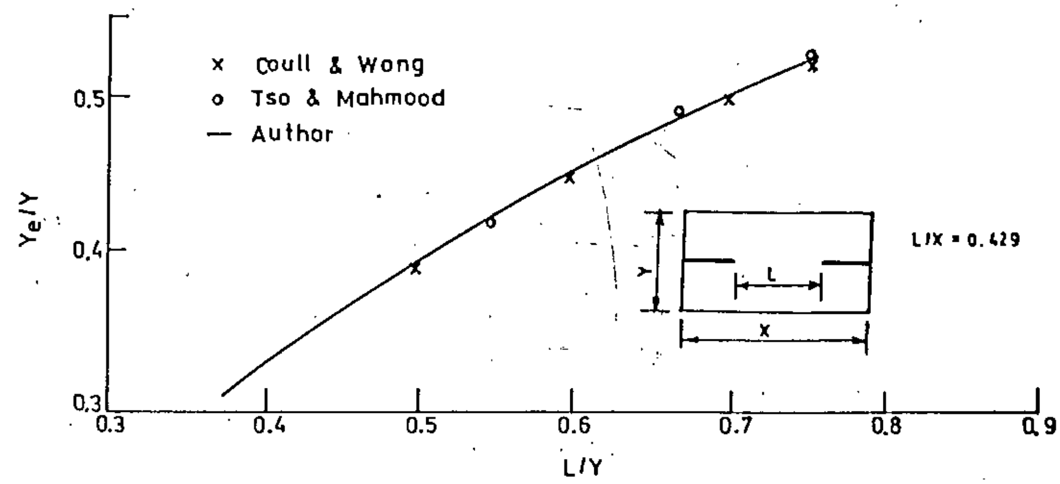

Fig. 4.2 Variation of effective width of a slab coupled with planar walls.

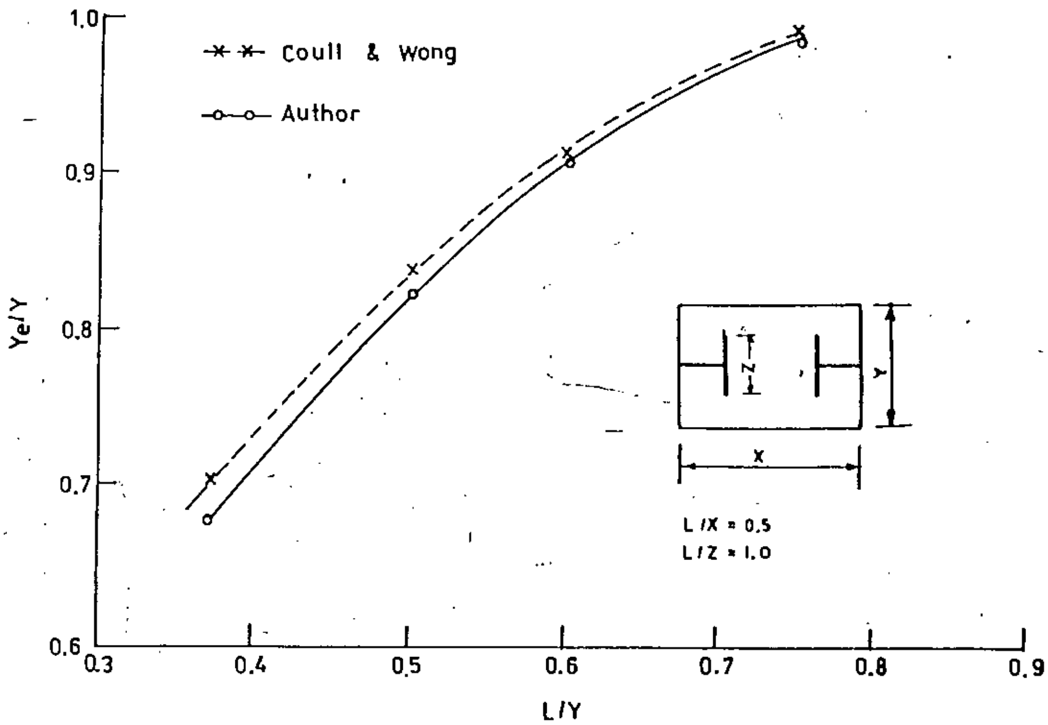

Fig. 4.3 Variation of effective width of a slab coupled with T-shaped walls.

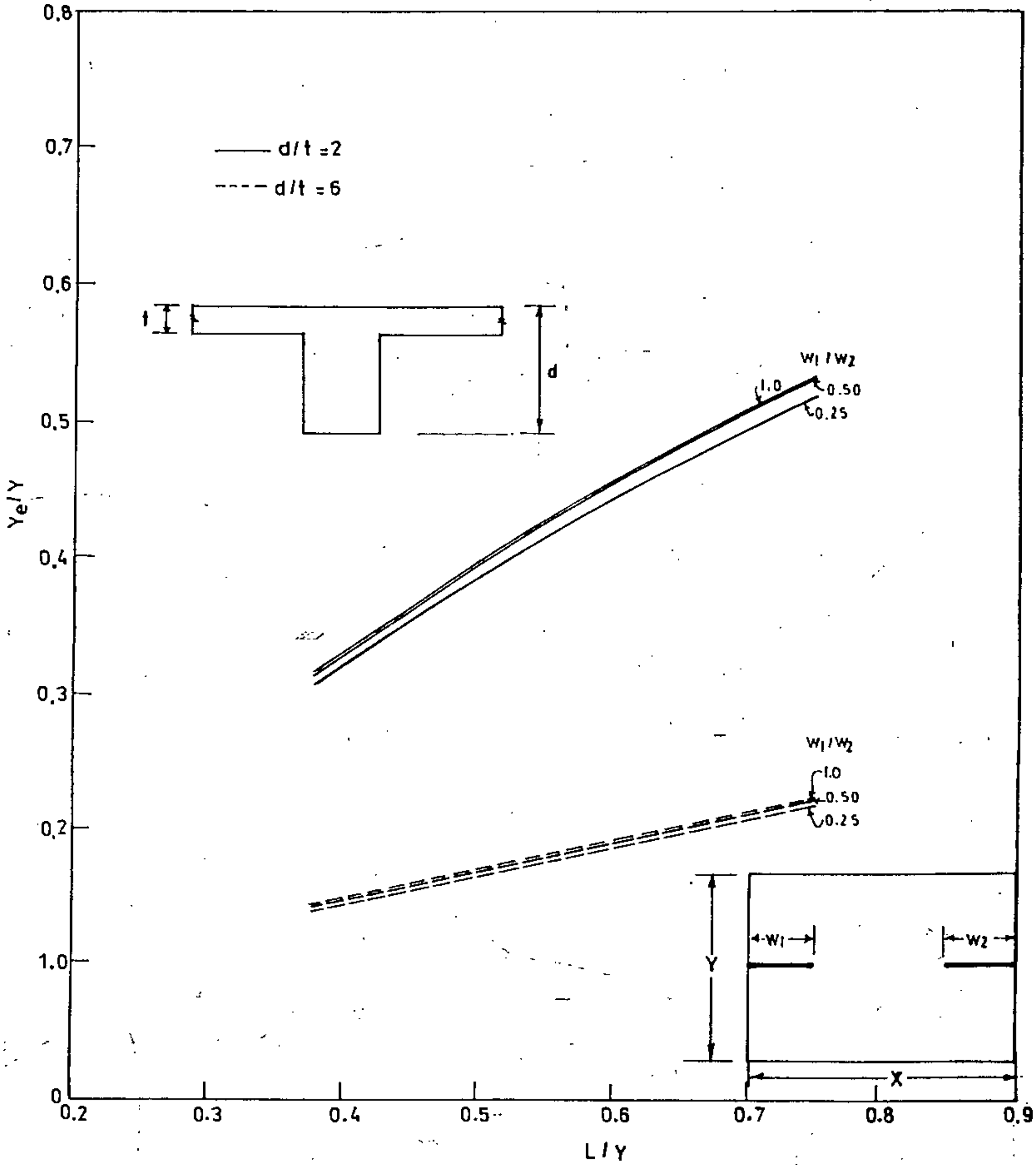

Fig. 4.4 Effect of unequal shear wall length in planar wall configuration.

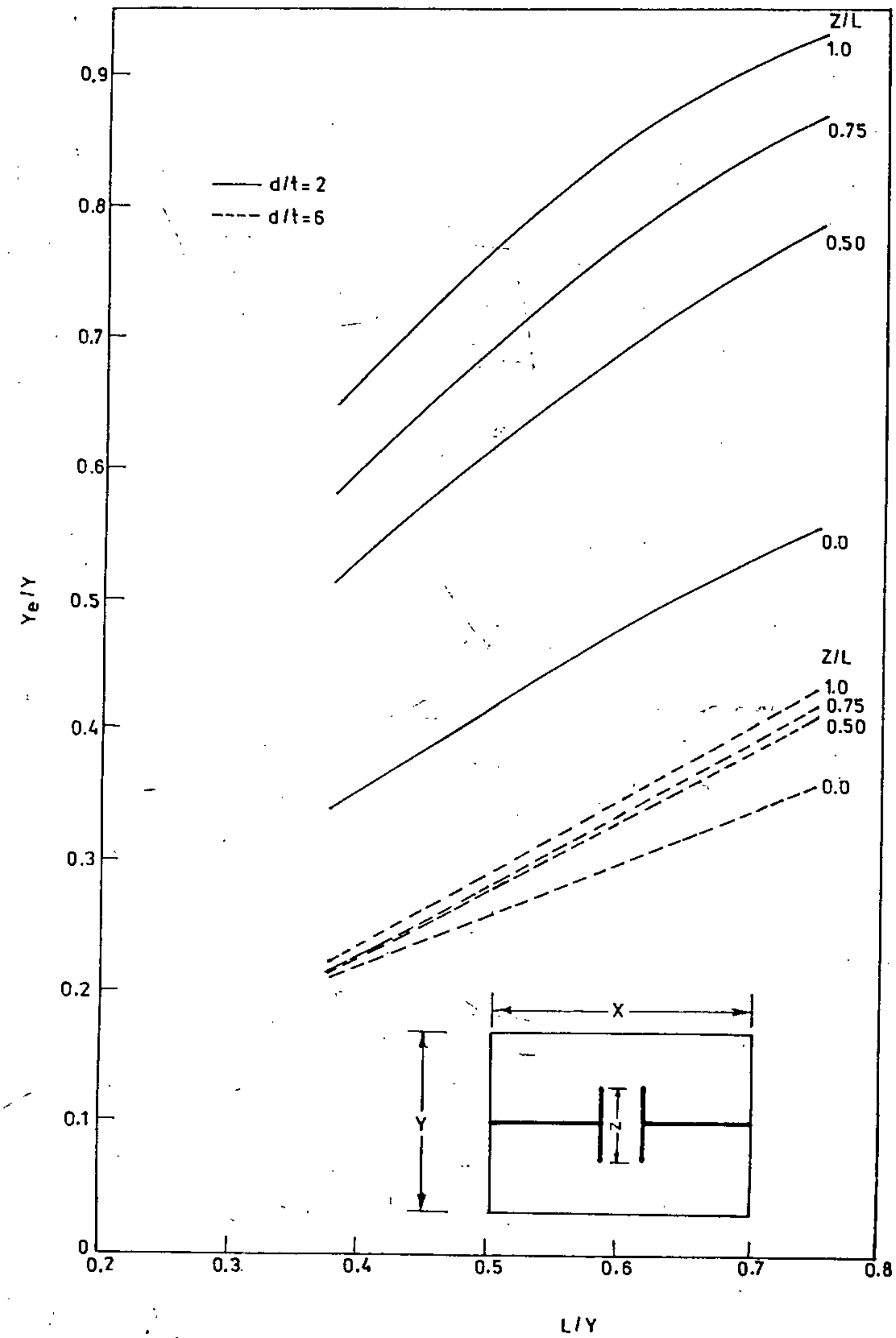

Fig. 4.5 Design curves for T-section walls configuration (L/X = 0.5).

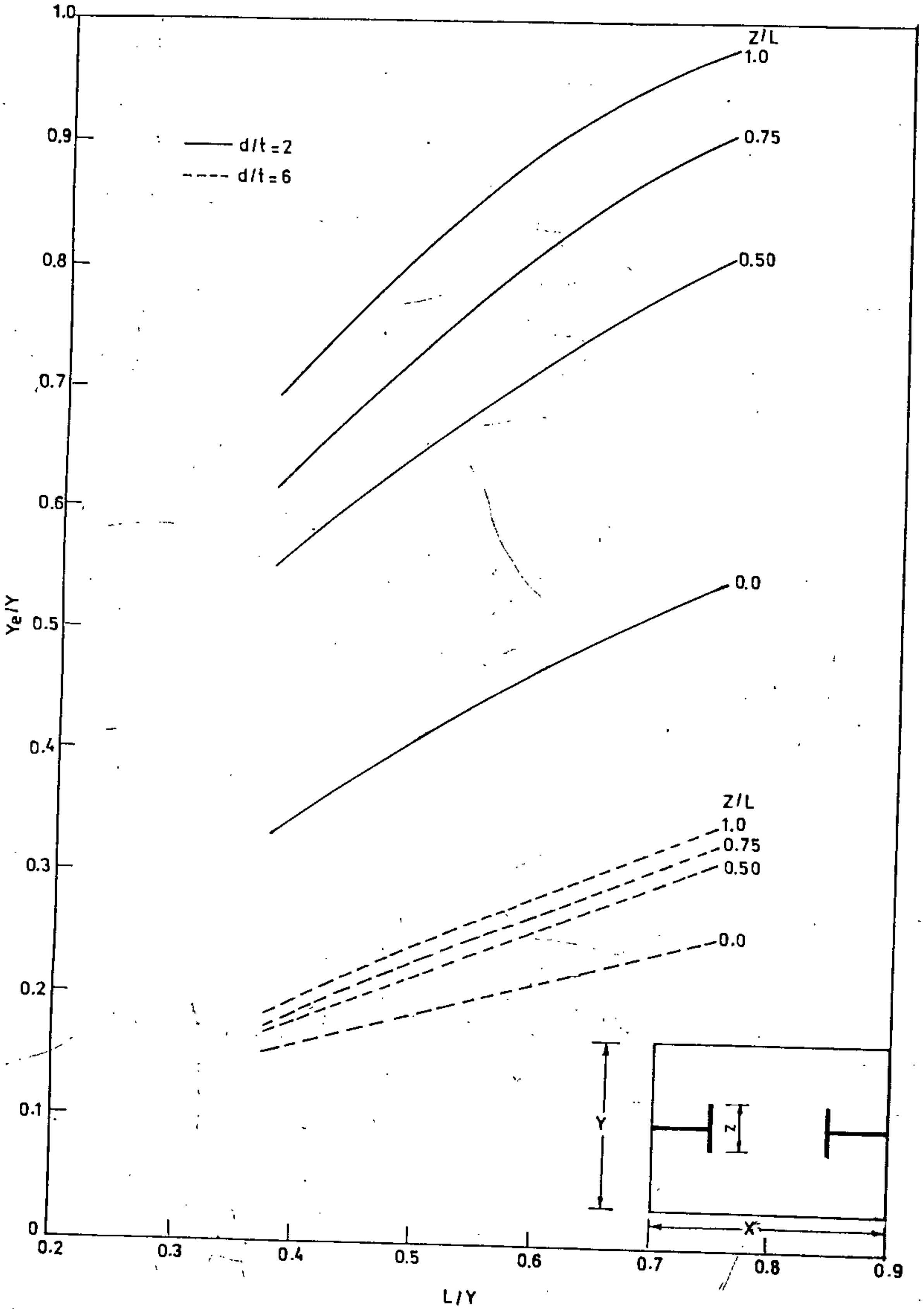

Fig. 4.6 Design curves for T-section walls configuration (L/X = 0.333).

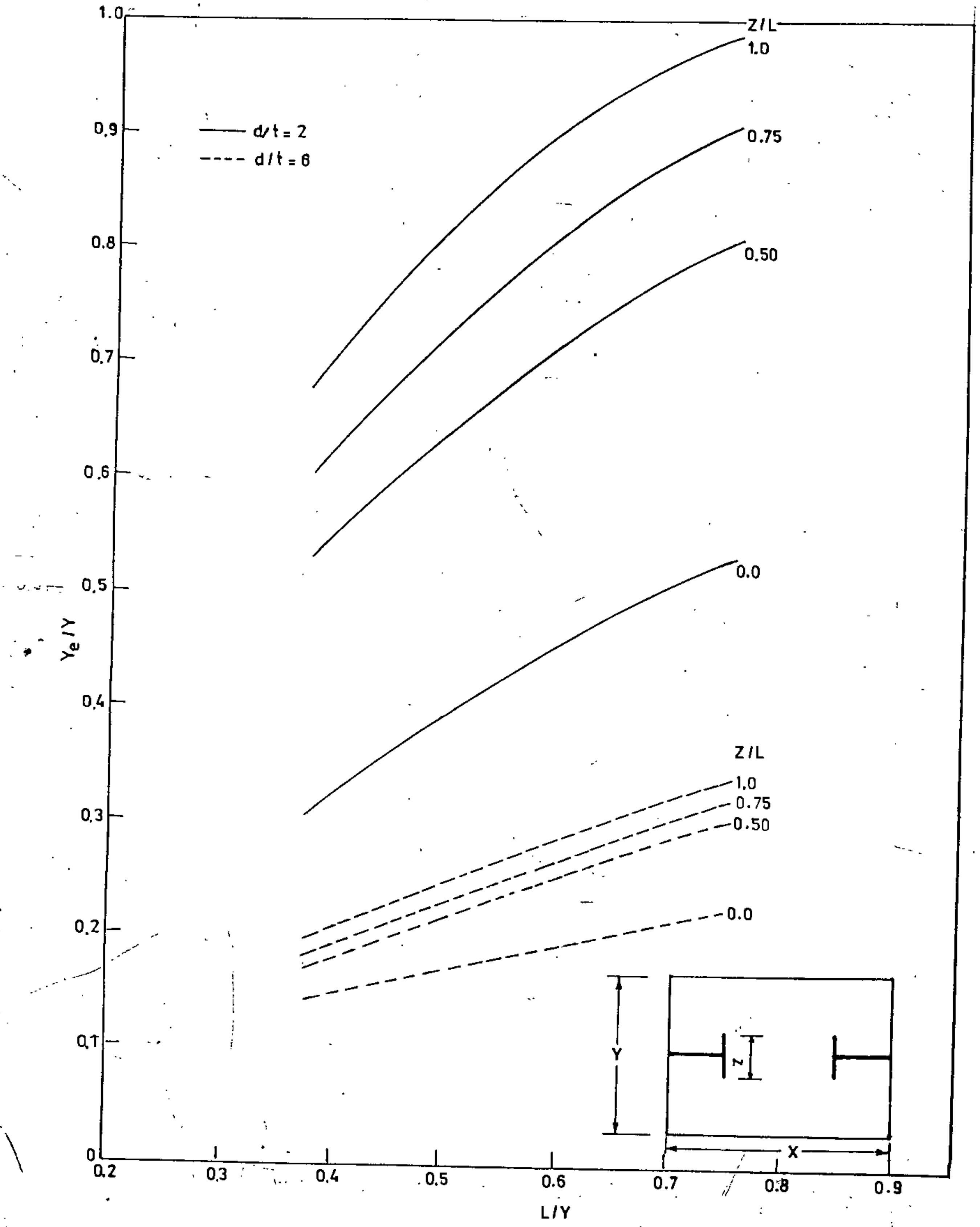

Fig. 4.7 Design curves for T-section walls configuration (L/X) = 0.15).

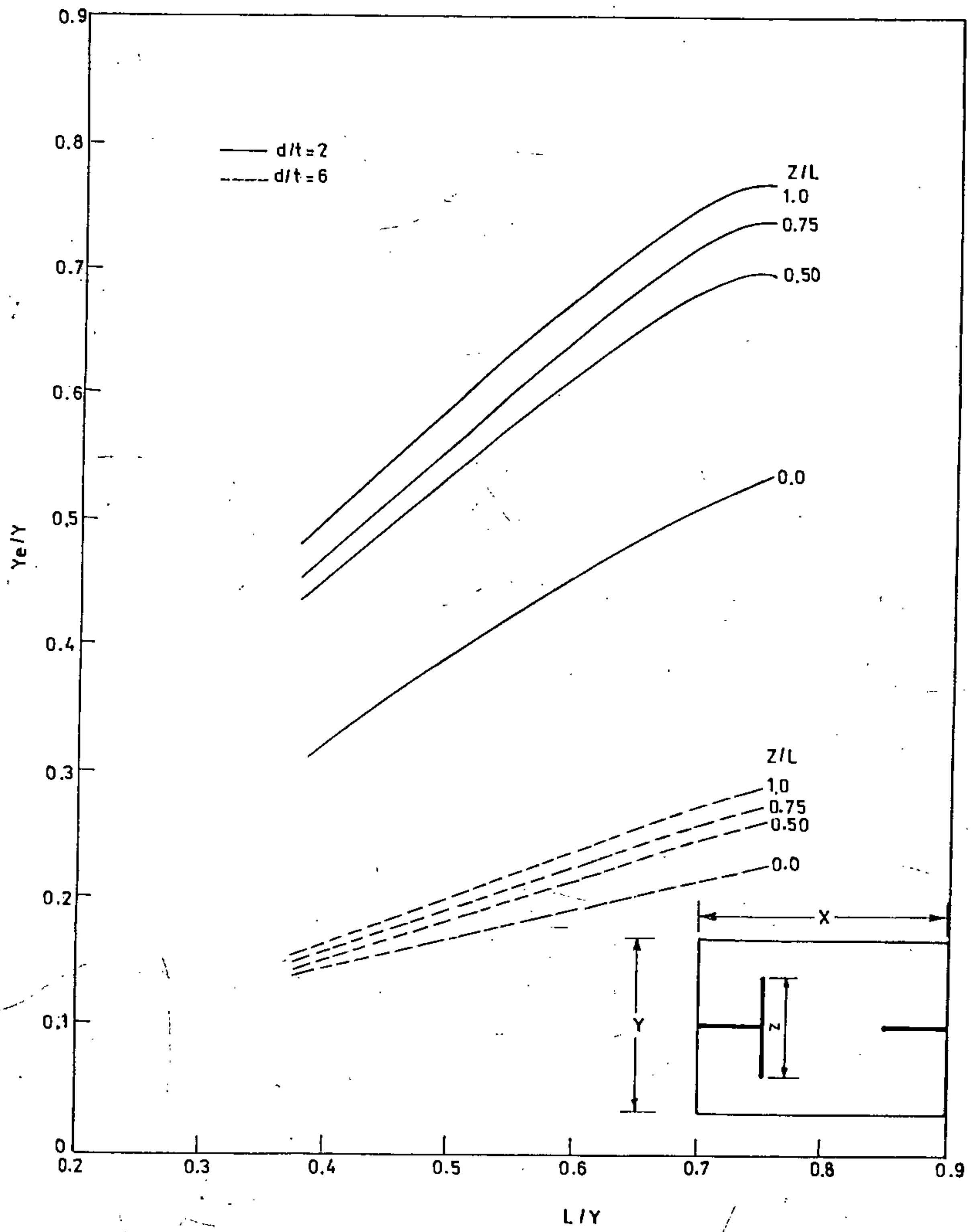

Fig. 4.8 Design curves for coupled planar and T-section walls.

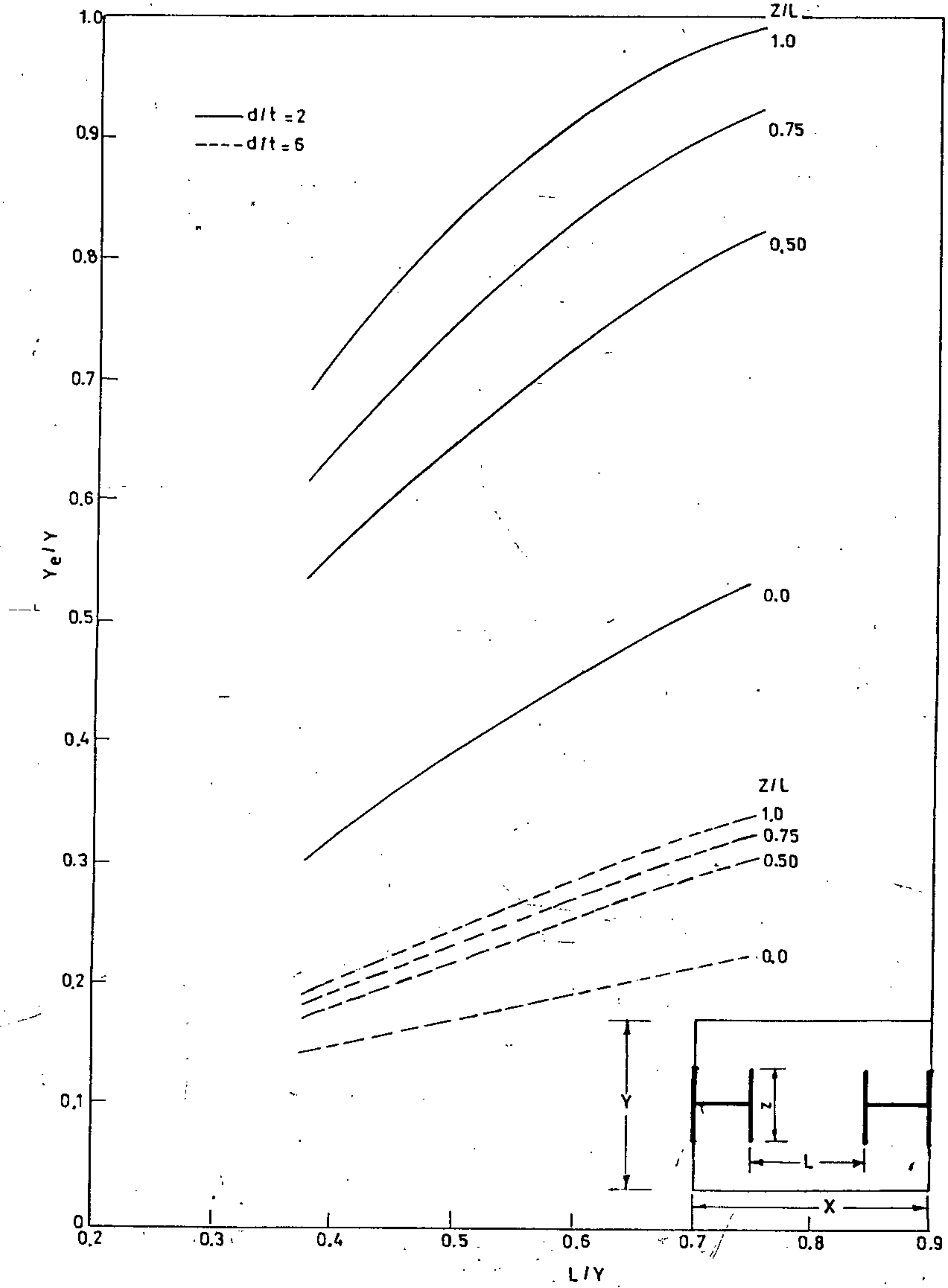

Fig. 4.9 Design curves for I-section walls.

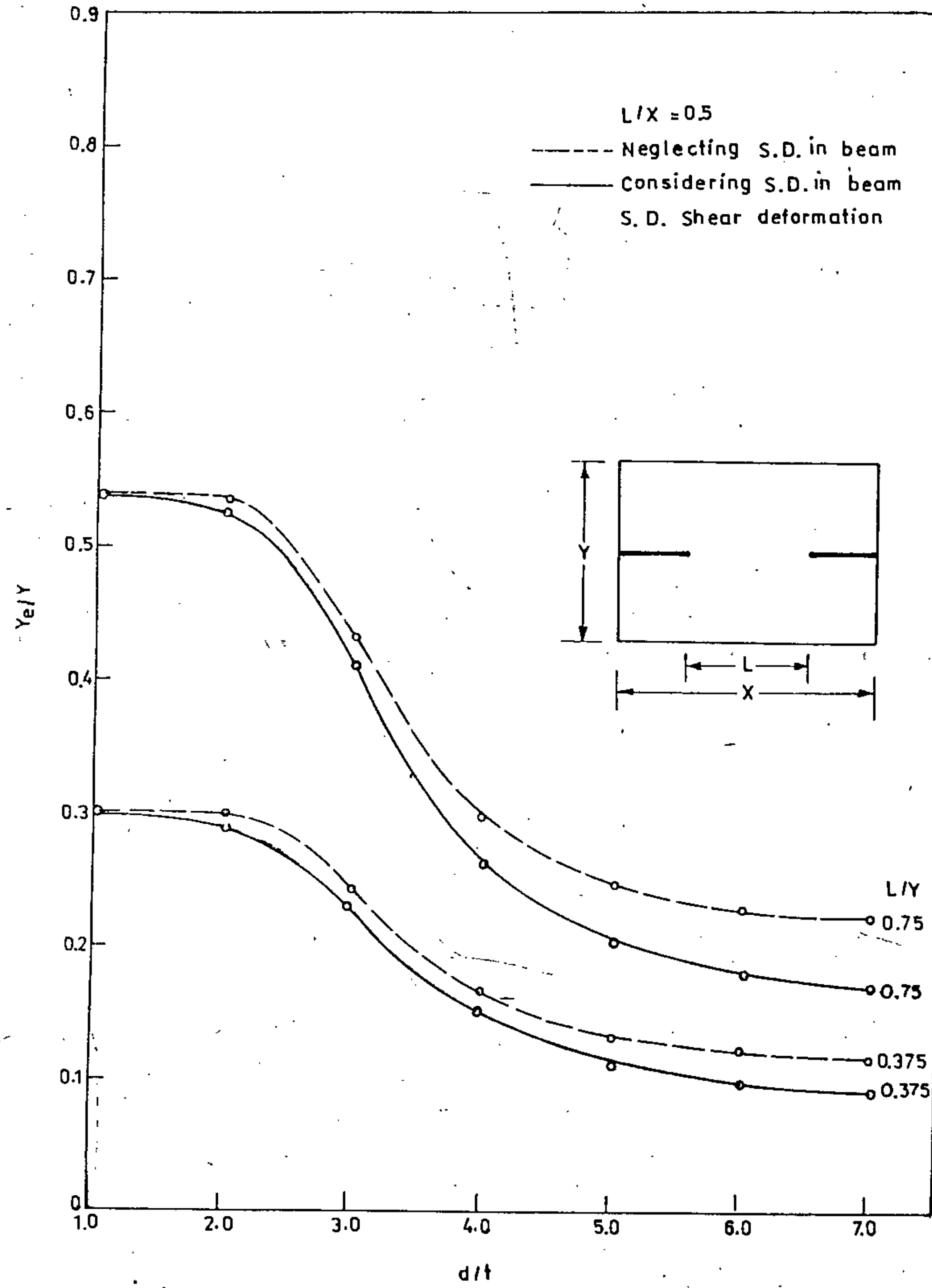

Fig. 4.10 Effect of beam depth in planar wall configuration.

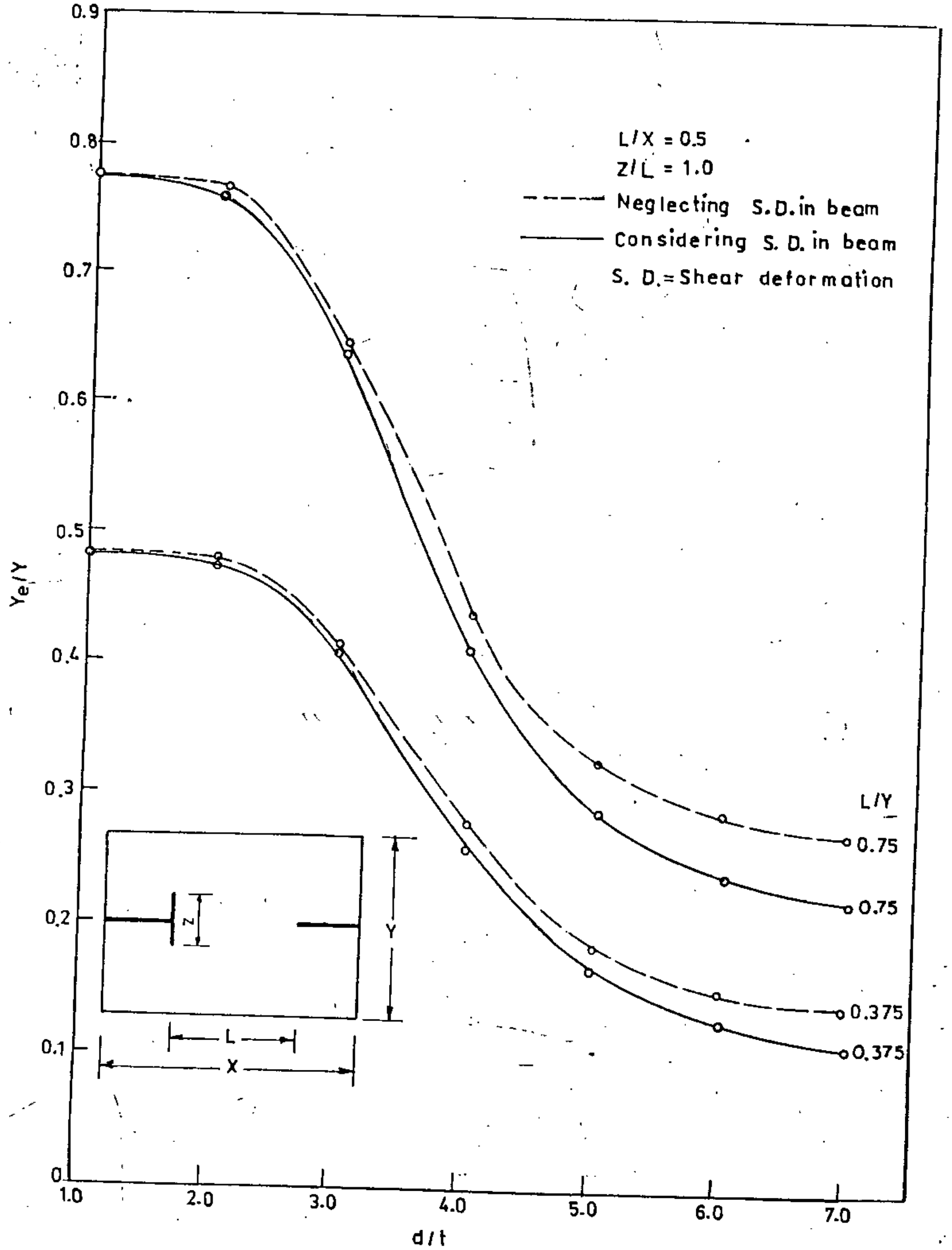

Fig. 4.11 Effect of beam depth in planar and T-section walls configuration.

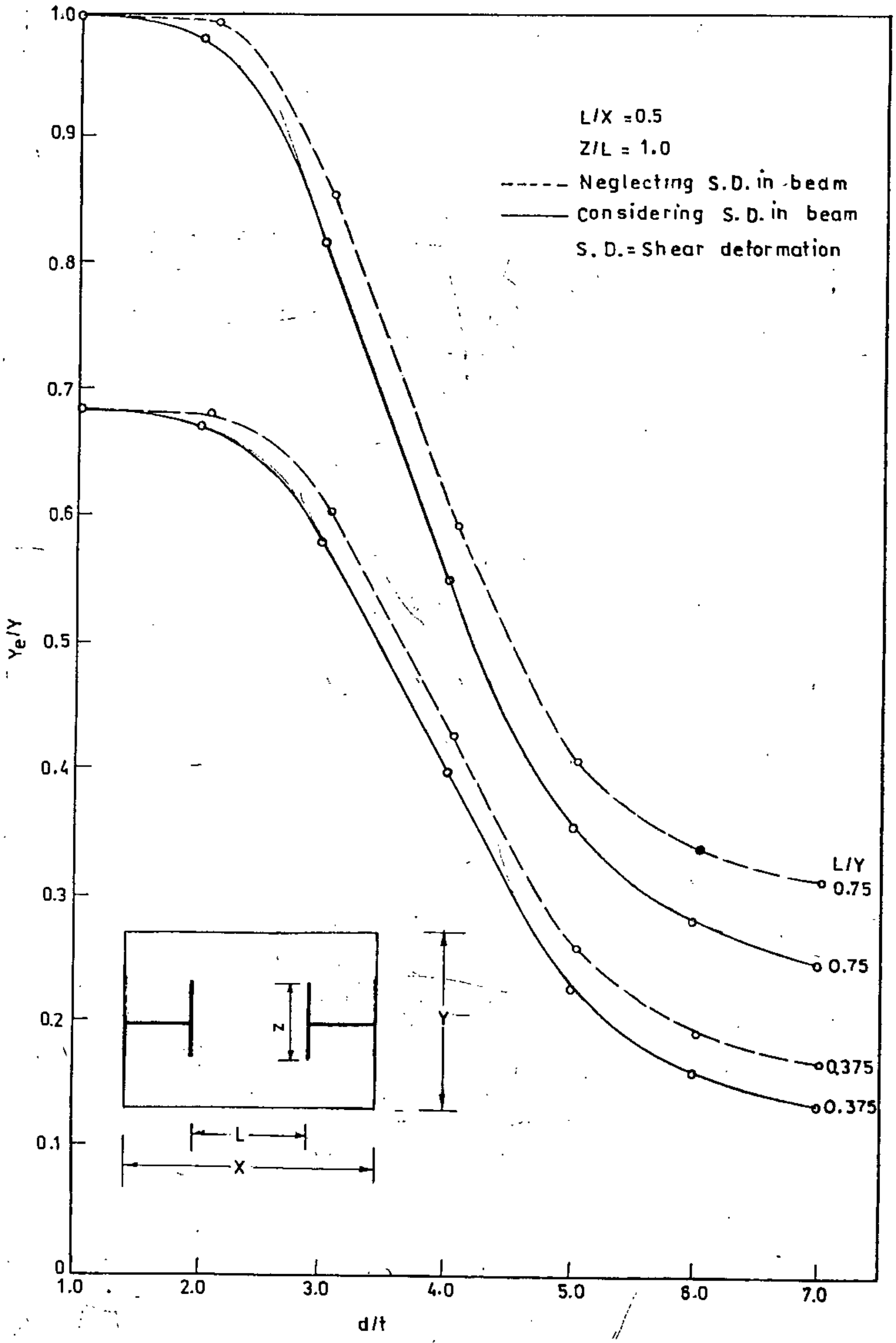

Fig. 4.12 Effect of beam depth in T-section walls configuration.

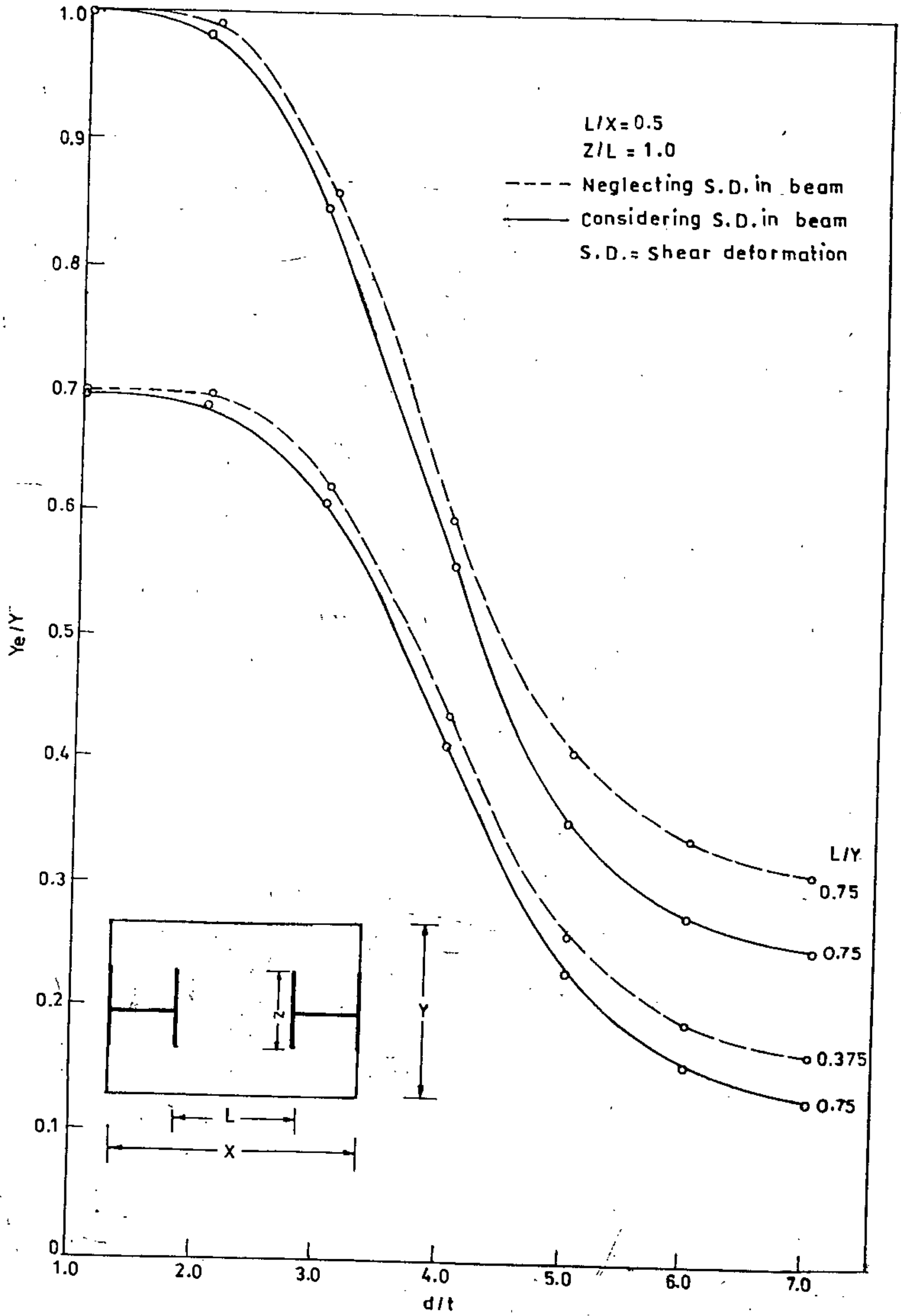

Fig. 4.13 Effect of beam depth in I-section walls configuration.

CHAPTER 5

CONCLUSIONS AND SUGGESTIONS FOR FURTHER STUDY

5.1 Conclusions

The composite action of beam and slab coupling a pair of shear walls has been investigated by a finite element method, and the relative influences of a range of structural parameters on the effective flange width of the composite coupling beam have been evaluated. Design curves for calculating the effective width have been provided for the normal range of structural dimensions encountered in practice. From the limited number of analyses, the following conclusions can be drawn.

i) For the coupled planar shear walls coupled by slab only the equation $Y_e/Y = L/Y\ (1-0.4\ L/Y)$; given by Coull and Wong[12] for calculating effective flange width can be used.

ii) Dissimilar wall lengths have little influence on the effective flange width of the connecting T-beam in coupled shear walls.

iii) Beyond certain depth of beam ($d/t > 6$), additional beam depth has almost negligible effect on the effective flange width for all the wall configurations considered, i.e two planar walls, two T-section walls, two I-section walls, one planar and other T-section wall.

Significant reductions in the wind stresses and deflections in the walls may be achieved by including the composite action when the lintel is relatively shallow.

iv) Interior flange length of flanged wall has the most significant effect on the effeftive width or slab and it has been observed that for I-section walls exterior flange have negligible effect on the effective flange width. Thus the corridor edge property have marked influence on the calculation of the effective flange width whereas exterior edge property of wall does not affect significantly on the same. Therefore it can be concluded that although the design charts are provided for one band of opening these can also be used for multiple bands of opening.

v) Shear deformation in the connecting beam reduces the effective slab width. In one of the extreme cases considered, consideration of shear deformation decreases the value of Y_e/Y from 0.22 to 0.17, for $L/Y = 0.75$ and $d/t = 7.0$ in planar wall configuration.

5.2 Suggestions for Further Study

To verify the results experimental investigation should be made.

To verify the inference that these results should hold equally good for coupled shear walls with multiple bands of opening, one should investigate a model of coupled shear walls theoretically and experimentally.

REFERENCES

1. Khan, F.R., Sbarounis, J.A. — 'Interaction of shear walls and frames', Journal of the Structure Division, Proc. ASCE, Vol. 90 No. ST 3 June 1964.

2. Barnard, P.R., Schwaighofer, J. — 'Interaction of shear walls connected solely through slabs', Ref. 21.

3. Choudhury, J.R. — Discussions Ref. 2.

4. Quadeer, A. — Discussion, Ref. 2.

5. Michael, D. — Discussions, Ref. 2.

6. Choudhury, J.R. — 'Analysis of plane and Spatial Systems of Interconnected Shear Walls', Ph.D. Thesis, University of Southampton, 1968.

7. Huq, M.M. — 'Flexural Stiffness of Floor Shear Wall Structures', M.Sc. Thesis, Bangladesh University of Engineering and Technology, 1974.

8. Quadeer, A. — 'The Bending Stiffness of Slabs Connecting Shear Walls', ACI Journal, Proc. Vol. 66 No. 6 June 1969.

9. Michael, D. — Discussions, ACI Journal No.12 Proc. Vol. 66, December 1969.

10. Pulmano, V.A. — 'Substructure Analysis of Multistory Flat Slab Buildings', Ref. 23.

11. Coull, A. — Discussions, Ref. 2.

12. Coull, A., Wong, Y.C. — 'Bending Stiffness of Floor Slabs in Cross-wall Structures', Proc. Instn. Civ. Engrs. Vol. 71, Part 2, London, Mar. 1981.

13. Coull, A., Wong, Y.C. — 'Composite Action Between Slabs and Lintel Beams', ASCE, Vol.110, ST No.3, March, 1984.

14. Adini, A., Clough, R.W. — Analysis of Plate Bending by the Finite Element Method. Rept. Submitted to the Nat. Sci. Foundation, Grant G7337, 1960.

15. Melosh, R. J. Basis of Deviation of Matrices for Direct Stiffness Method, Jnl. A.I.A.A., Vol. 1, pp. 1631-1637, 1963.

16. Jenkins, W.M. Harrison, T. Analysis of Tall Buildings with Shear Walls under Bending and Torsion, pp. 413-444, Ref. 18.

17. Zienkiewicz, O.C. Cheung, Y.K. 'Finite Element Method of Analysis for Arch Dam Shells and Comparison with Finite Difference Procedures', Proceedings of Symposium on Theory of Arch Dams, Southampton Univ.; 1968.

18. Clough, R.W. Tocher, J.L. 'Analysis of Thin Arch Dams by the Finite Element Methods', Proceedings of Symposium on Theory of Arch Dams, Southampton University, 1964.

19. Bathe, K.J. Wilson, E.L. 'Formulation and Calculation of Isoparametric Finite Element Matrices', Chap. 4, Numerical Methods in Finite Element Analysis, 1976, Published by Prentice-Hall, Inc., Englewood Cliffs, New Jersey.

20. Clough, R.W. Tocher, J.L. 'Finite Element Stiffness Matrices for Analysis of Plates in Bending, Proc. Conf. Matrix Methods in Struct. Mech., AN Force Inst. of Tech., Wright Patterson A.F. Base, Ohio, 1965.

21. Coull, A. Smith, B.S. 'Tall Buildings' with Particular Reference to Shear Wall Structures. Proc. of a Symposium Held at the University of Southampton (1966) Pergamon Press, 1967.

22. Tso, W.K. Mahmoud, M.A. 'Effective Width of Coupling Slabs in Shear Wall Buildings', J. Struct. Div. Am. Soc. Civ. Engrs., 1977, 103, ST 3, Mar., 573-586.

23. 'Proceedings of the Regional Conference Tall Buildings, Bangkok, January, 1974.

APPENDIX-A

CATALOGUE OF STIFFNESS MATRICES

I. Stiffness matrix for a Rectangular Plate Bending Element.

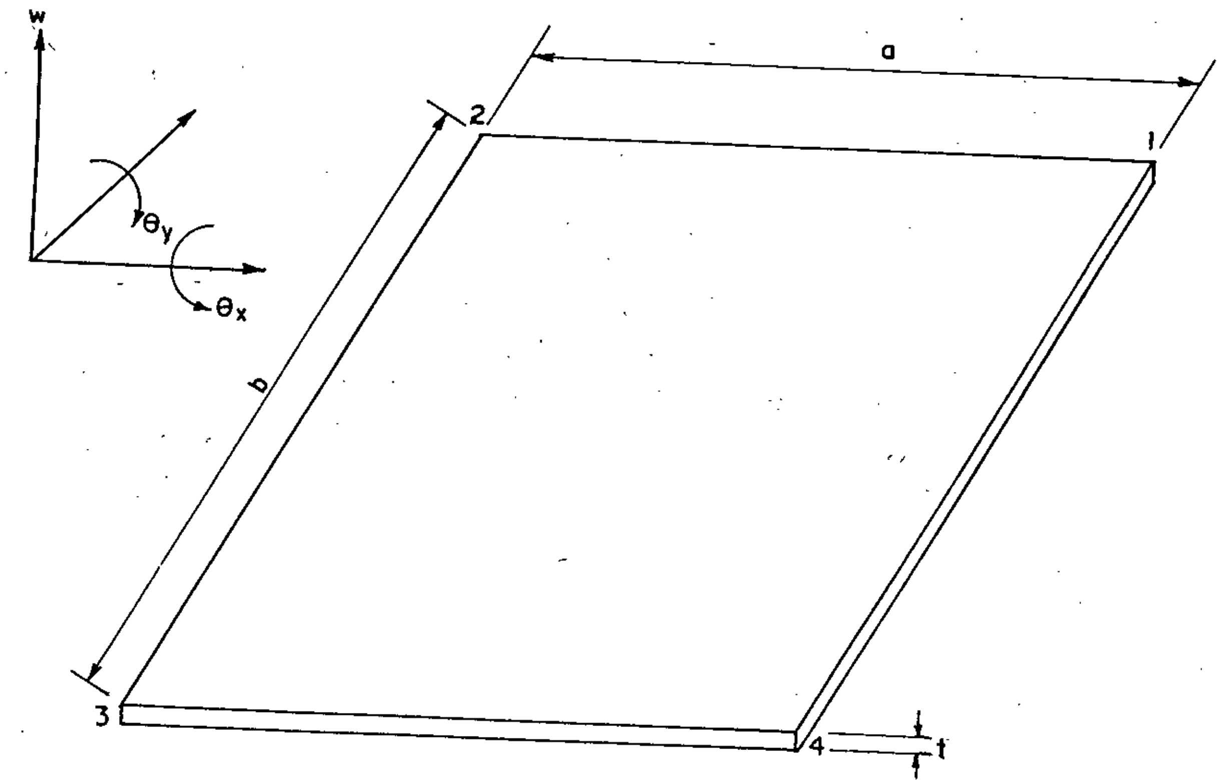

Displacement function: $w = a_1 + a_2x \pm a_3y + a_4x^2 + a_5xy$

$$+ a_6y^2 + a_7x^3 + a_8x^2y + a_9xy^2 + a_{10}y^3$$

$$+ a_{11}x^3y + a_{12}xy^3$$

Displacement vector: $\underline{d} = w_1 \;\theta_{x,1} \;\theta_{y,1} \;w_2 \;\theta_{x,2} \;\theta_{y,2}$

$$w_3 \;\theta_{x,3} \;\theta_{y,3} \;w_4 \;\theta_{x,4} \;\theta_{y,4}$$

The generalized element stiffness matrix $\underline{k}$ for the rectangular plate of 12 degree of freedom is given below. All elements of this matrix

$$(\underline{k})_{ij} \equiv (i, j)$$

which are different from zero are listed for the case of isotropic material and constant element thickness. The indices i,j denote row and column number respectively.

Since $\underline{k}$ is a symmetrical matrix, only the elements on and below the main diagonal are given.

The following symbols are used

β = b/a

ν = Poisson's ratio

$\overline{MF}$ = $14-4\nu$

MO = $1 + 4\nu$

MM = $1 - \nu$

BTI = $\beta^2 + \beta^{-2}$

N.B: All expressions must be multiplied by

$$\frac{Et^3}{12(1-\nu^2)\,ab}$$

$(1,1) = 4BTI + MF/5$

$(2,1) = -(2\beta^{-2} + MO/5)\,b$

$(3,1) = (2\beta^2 + MO/5)\,a$

$(7,1) = 2BTI + MF/5$

$(8,1) = (-\beta^{-2} + MM/5)\,b$

$(9,1) = (\beta^2 - MM/5)\,a$

$(2,2) = (4\beta^{-2}/3 + 4MM/15)\,b^2$

$(3,2) = -\nu ab$

$(4,2) = (-\beta^{-2} + MO/5)\,b$

$(5,2) = (2\beta^{-2}/3 - 4MM/15)\,b^2$

$(7,2) = (\beta^{-2} - MM/5)\,b$

$(8,2) = (\beta^{-2}/3 + MM/15)\,b^2$

$(10,2) = (2\beta^{-2} + MM/5)\,b$

$(11,2) = (2\beta^{-2}/3 - MM/15)\,b^2$

$(3,3) = (4\beta^{2}/3 + 4MM/15)\,a^2$

$(4,3) = -(2\beta^{2} + MM/5)\,a$

$(6,3) = (2\beta^{2}/3 - MM/15)\,a^2$

$(7,3) = (-\beta^{2} + MM/5)\,a$

$(9,3) = (\beta^{2}/3 + MM/15)\,a^2$

$(10,3) = (\beta^{2} - MO/5)\,a$

$(11,3) = (2\beta^{2}/3 - 4MM/15)\,a^2$

$(4,4) = 4BTI + MF/5$

$(5,4) = -(2\beta^{-2} + MO/5)\,b$

$(6,4) = -(2\beta^{2} + MO/5)\,a$

$(7,4) = 2(\beta^{2} - 2\beta^{-2}) - MF/5$

$(8,4) = -(2\beta^{-2} + MM/5)\,b$

$(9,4) = (-\beta^{2} + MO/5)\,a$

$(10,4) = -2BTI + MF/5$

$(11,4) = (-\beta^{-2} + MM/5)\,b$

$(12,4) = (-\beta^{2} + MM/5)\,a$

$(5,5) = (4\beta^{-2}/3 + 4MM/15)\,b^2$

$(6,5) = \nu ab$

$(7,5) = (2\beta^{-2} + MM/5)\,b$

$(8,5) = (2\beta^{-2}/3 - MM/15)\,b^2$

$(10,5) = (\beta^{-2} - MM/5)\,b$

$(12,5) = (\beta\beta^{-2}/3 + MM/15)\,b^2$

$(6,6) = (4\beta^{2-}/3 + 4MM/15)\,a^2$

$(7,6) = (-\beta^2 + MO/5)\,a$

$(9,6) = (2\beta^2/3-4mm/5)\,a^2$

$(10,6) = (\ \beta^2 - MM/5)\,a$

$(12,6) = (\ \beta^2/3+MM/15)\,a^2$

$(7,7) = 4BTI+MF/5$

$(8,7) = -(2\beta^2 + MO/5)\,b$

$(9,7) = -(2\beta^2 + MO/5)\,a-$

$(10,7) = -2(2\beta^2-\beta^{-2}) - MF/5$

$(11,7) = (\beta^{-2} - MO/5)\,b$

$(12,7) = -(2\beta^2 + MM/5)\,a$

$(8,8) = (4\beta^{-2}/3 + 4MM/15)\,b^2$

$(9,8) = -\nu ab$

$(10,8) = (\beta^{-2} - MO/5)\,b$

$(11,8) = (2\beta^{-2}/3-4MM/15)\,b^2$

$(9,9) = (4\beta^2/3+4MM/15)\,a^2$

$(10,9) = (2\beta^2 + MM/5)\,a$

$(12,9) = (2\beta^2/3-MM/15)\,a^2$

$(10,10) = 4BTI + MF/5$

$(11,10) = (2\beta^{-2} + MO/5)\,b$

$(12,10) = (2\beta^2 + MO/5)\,a$

$(11,11) = (4\beta^{-2} + 4MM/15)\,b^2$

$(11,12) = \nu ab$

$(12,12) = (4\beta^2/3 + 4MM/15)\,a^2$

$(4,1) = -2(2\beta^2 - \beta^{-2}) - MF/5$

$(5,1) = (-\beta^{-2} + MO/5)\,b$

$(6,1) = (2\beta^2 + MM/5)\,a$

$(10,1) = 2(\beta^2 - 2\beta^{-2}) - MF/5$

$(11,1) = -(2\beta^{-2} + MM/5)\,b$

$(12,\ 1) = (\beta^2 - MO/5)\,a$

II. Stiffness Matrix for Beam Element

(neglecting shear deformation)

Since $\underline{k}$ is a symmetric matrix, only the element on and above the main diagonal which are different from zero are given

OX DIRECTION

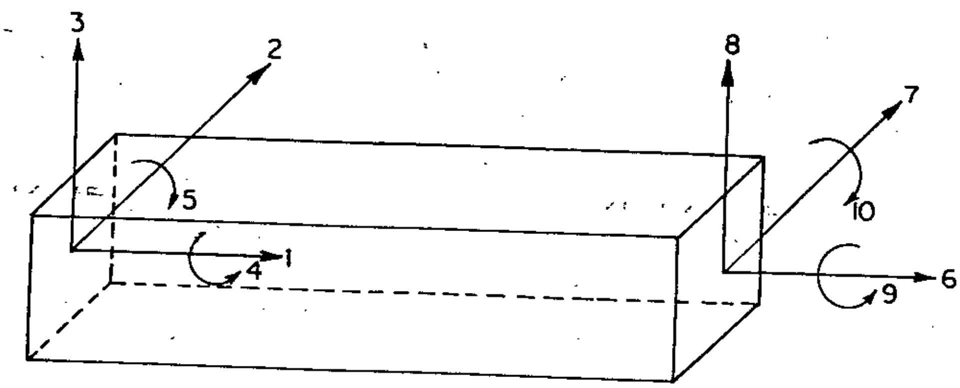

The following symbols are used:

E = Young's Modulus

A = Cross-sectional area

L = Length of beam element

I_y = Moment of inertia about Y-axis

I_z = Moment of inertia about z-axis

J = Polar moment of inertia

G = Shear Modulus

$(1,1) = AE/L$

$(2,2) = 12\ EI_z/L^3$

$(3,3) = 12\ EI_y/L^3$

$(4,4) = GJ/L$

$(5,5) = 4\ EI_y/L$

$(3,5) = -\dfrac{6EI_y}{L^2}$

$(6,6) = AE/L$

$(7,7) = 12\ EI_y/L^3$

$(8,8) = 12\ EI_y/L^3$

$(9,9) = GJ/L$

$(10,10) = 4\ EI_y/L$

$(8,10) = \dfrac{6EI_y}{L^2}$

$(1,6) = -\ AE/L$

$(2,7) = -\ 12\ EI_z/L^3$

$(4,9) = -\ GJ/L$

$(5,10) = 2\ EI_y/L$

$(3,10) = -\dfrac{6EI_y}{L^2}$

$(5,8) = \dfrac{6EI_y}{L^2}$

θY DIRECTION

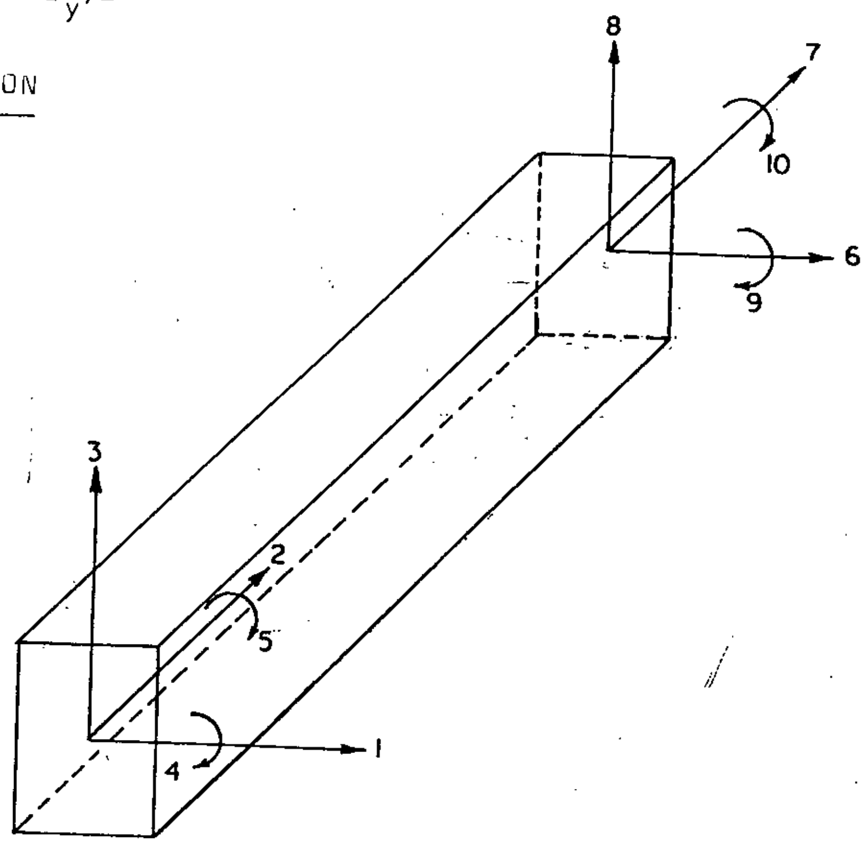

$(1,1) = 12EI_z/L^3$

$(2,2) = AE/L$

$(3,3) = 12\ EI_x/L^3$

$(4,4) = 4EI_x/L$

$(5,5) = GJ/L$

$(3,4) = 6EI_x/L^2$

$(6,6) = 12EI_z/L^3$

$(7,7) = AE/L$

$(8,8) = 12E_{\bar{x}}/L^3$

$(9,9) = 4EI_x/L$

$(10,10) = GJ/L$

$(8,9) = -\ 6EI_x/L^3$

$(1,6) = -12EI_z/L^3$

$(2,7) = -AE/L$

$(3,8) = -\ 12EJ_x/L^3$

$(5,10) = -\ GJ/L$

$(4,9) = 2EI_x/L$

$(3,9) = 6EI_x/L^2$

$(4,8) = -\ 6EI_x/L^2$

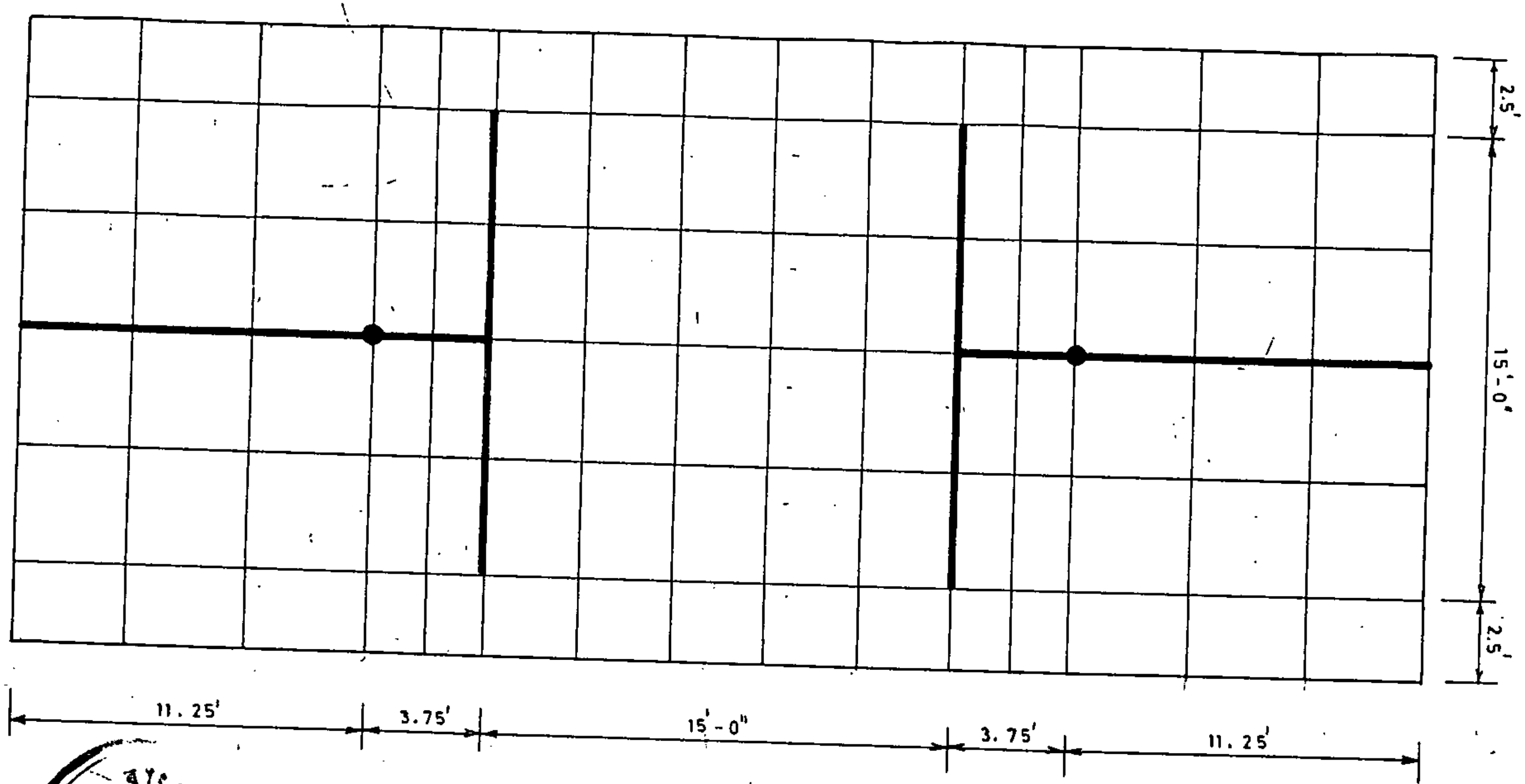

Finite element idealization of floor slab